CHOLERA BACTERIA DETECTION SYSTEM

A Thesis

Presented to the

Faculty of

California State Polytechnic University, Pomona

In Partial Fulfillment

Of the Requirements for the Degree

Master of Science

In

Electrical Engineering

By

Darya Moshrefi

2017

SIGNATURE PAGE

THESIS: CHOLERA BACTERIA DETECTION SYSTEM

AUTHOR: Darya Moshrefi

DATE SUBMITTED: Fall 2017

Electrical and Computer Engineering Department

Dr. Brita Olson _____
Thesis Committee Chair
Electrical and Computer Engineering

Dr. Norali Pernalete _____
Electrical and Computer Engineering

Dr. James Kang _____
Electrical and Computer Engineering

ABSTRACT

Cholera is an acute and deadly disease that is spread all around the world through contaminated water and food. Vibrio Cholerae bacterium causes infection in small intestine. If detected early, Cholera can be cured. Current detection methods require laboratory equipment, long processing time and in some cases, are not accurate enough. The purpose of this thesis is to extend an innovative bacteria detection platform by integrating necessary support electronics onto a same CMOS chip and to use an inherited property of Vibrio Cholerae bacterium's cell, for an accurate, low cost, low power and highly miniaturized lab system-on-a chip. In this way moving this technology closer to practical third world use.

TABLE OF CONTENTS

SIGNATURE PAGE ii
ABSTRACT iii
LIST OF FIGURES v
CHAPTER 1 1
Cholera 1
Treatment 2
Detection 2
CHAPTER 2 6
Vibrio Cholerae, A Magnetotactic Bacterium 6
AN INNOVATIVE DETECTION SYSTEM 7
The Prototype 11
Advantages 14
Shortcomings 14
CHAPTER 3 15
Bacteria Detection Platform 15
THE DETECTION CIRCUIT COMPONENTS 17
Current Reference 17
Bandgap Voltage Reference 23
LDO: Low Dropout Voltage Regulator 27
Ring Oscillator 32
Detection Circuit 35
Two-Stage Operational Amplifier 39
Low Pass Filter 43
Decision Circuit 45
CONCLUSION 47
REFERENCES 48

LIST OF FIGURES

Figure 1: Spread of Cholera around the world 2010-2015 [3]..... 1

Figure 2:Vibrio Cholerae on TCBS agar vs. different bacteria [9]..... 3

Figure 3:Magnetotactic bacteria and Magnetosomes [13]..... 6

Figure 4:Proposed design by Ecole Polytechnique de Montreal, Canada [14]..... 8

Figure 5: The chamber with the microelectrode arrays [15]..... 9

Figure 6: Stacked microelectrode pairs [15]..... 10

Figure 7: Circuit model of an electrode pair [15] 10

Figure 8: In operation a DC current Iref is injected into the sample causing the voltage across the sample to increase. The nature of the increase depends on the value of Rsol and thus the presence of bacteria. 11

Figure 9: Diagram of detection system [15] 12

Figure 10: V_140K and V_100K show the input to the amplifier and corresponding outputs for different values of Rsol [15]..... 13

Figure 11: Block Diagram of designed bacteria detection system 15

Figure 12: Current reference schematic..... 17

Figure 13: Input and Output currents block diagram..... 18

Figure 14: Changes in output current relative to change in input current 18

Figure 15: Temperature coefficient of VBE current reference..... 22

Figure 16: VBE Current reference's voltage compliance 22

Figure 17: Bandgap voltage reference schematic 23

Figure 18: Temperature independent voltage reference 24

Figure 19: Temperature coefficient of voltage reference 25

Figure 20: NPN Darlington pass element 27

Figure 21: LDO’s Diagram 28

Figure 22: LDO's schematic 29

Figure 23: LDO's gain and phase margin Bode plots 30

Figure 24: LDO's Vout vs. Supply voltage 31

Figure 25: CMOS inverter 32

Figure 26: Inverter symbol 32

Figure 27: Ring oscillator schematic 33

Figure 28: Input and output signals of the ring oscillator 34

Figure 29: The main detection circuit 35

Figure 30: Detection circuit schematic with 2 different detected resistances 37

Figure 31: Detection output with and without the inverter 38

Figure 32: Operational amplifier's schematic 39

Figure 33: Low pass filter 43

Figure 34: DC content of the detection signals 44

Figure 35:RC low pass filter Bode plots 44

Figure 36: The comparator schematic 45

Figure 37: Decision circuit’s output 46

CHAPTER 1

Cholera

Cholera is an acute and often fatal disease caused by infection of the small intestine with the bacterium Vibrio Cholerae. The disease causes profuse diarrhea and vomiting resulting in rapid loss of body fluids. If left untreated, it can lead to severe dehydration, shock and death in a matter of hours.

Cholera is spread through contaminated water and food. The disease can spread rapidly in areas with inadequate sewage and drinking water.

According to the centers for disease control and prevention an estimated 3-5 million cases and over 100,000 deaths occur every year around the world. [1]

The Global Health Observatory (GHO) data shows major Cholera outbreak epidemics affecting several areas including the Central and West Africa, Papua New Guinea in the pacific region, Asia and the Americas. [3]

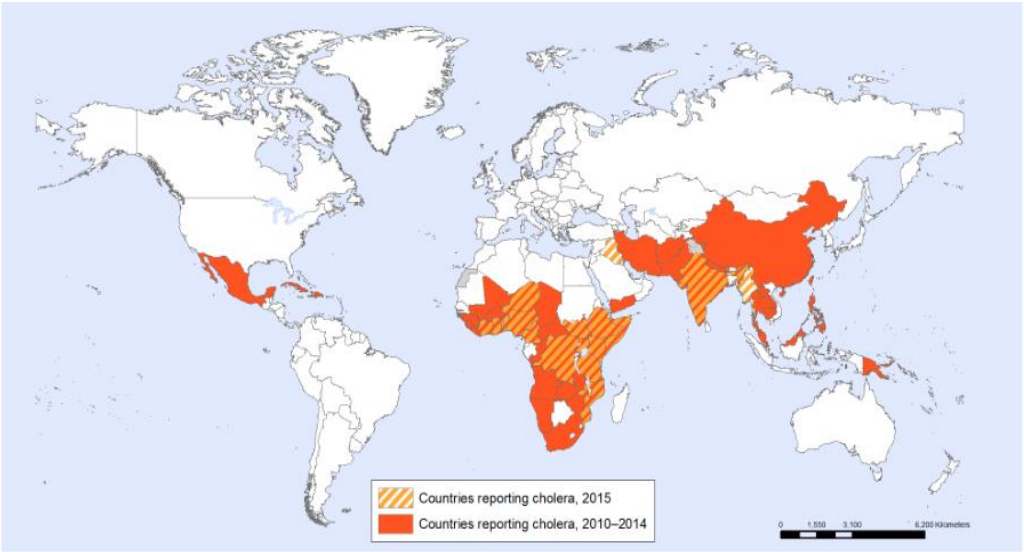

Figure 1: Spread of Cholera around the world 2010-2015 [3]

In July 2017 the world health organization described the cholera outbreak in Yemen as the worst cholera outbreak in the world. As of September 2017, more than 2000 cholera related deaths have been reported. The International Red Cross predicts over 1 million cholera cases in Yemen by end of 2017. [16]

In 2010, Cholera killed about 10,000 people in Haiti only months after the deadly earthquake devastated the area. [1]

Treatment

Rehydration is the main goal of Cholera treatment. The patient needs to regain the lost fluid and electrolytes promptly. A simple rehydration solution, oral rehydration salt (ORS) can provide the necessary treatment. In severe cases, intravenous fluids are needed. Antibiotics injection is not necessary to treat Cholera; however, the effect of these drugs on reducing the duration of Cholera related diarrhea has been positive. Taking Zinc supplements has also proven to be helpful in shortening the illness period in children with cholera. [5]

Detection

Detection, isolation and identification of Vibrio Cholerae bacterium are crucial for diagnosis of the disease. There are several applied and proposed methods to detect cholera, but each involve tradeoffs between speed, cost, accuracy, etc.…

Bacteria Culture Method

The most common method used in the field is culturing the bacteria. Samples are taken from the patient using a sterile cotton bud. The sample is then placed on a plate containing TCBS (Thiosulfate Citrate Bile salts) agar, a selective medium that isolates the bacteria from the diarrhea. [7] TCBS agar is green when prepared. Overnight growth

(18 to 24 hours) of Vibrio Cholerae will produce large (2 to 4 mm in diameter), slightly flattened, yellow colonies with opaque centers and translucent peripheries as shown in figure 2. The yellow color is caused by the fermentation of sucrose in the medium. The clumps are then analyzed to detect the exact strain of cholera. This definitive diagnosis allows cholera to be distinguished from other bacterial, or viral causes of dysentery. [8]

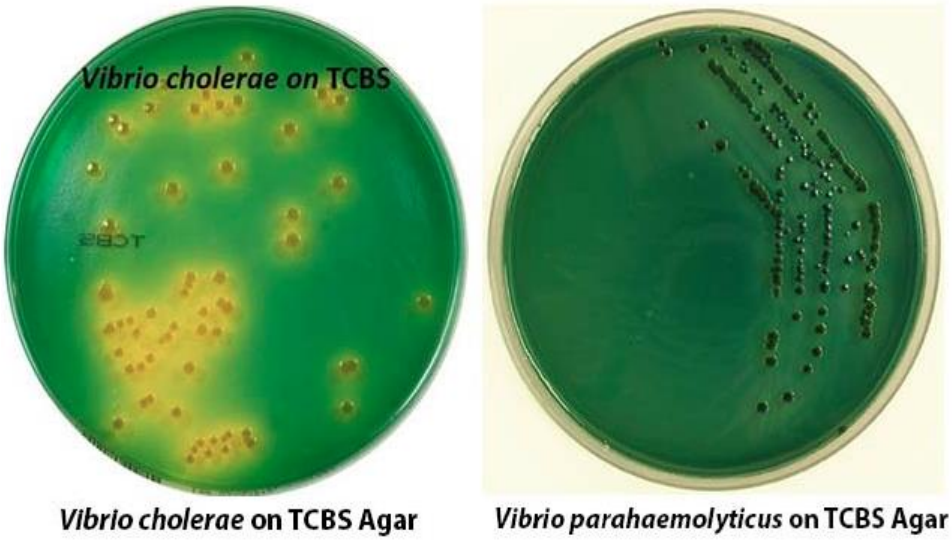

Figure 2:Vibrio Cholerae on TCBS agar vs. different bacteria [9]

Although this method provides a definitive diagnosis, it takes a long time to be processed and in severe cases of cholera time is of the essence. The need for access to laboratory equipment and well-trained personnel also make this method not feasible in remote, poor areas where major cholera epidemic occurs.

Flow Cytometry and Fluorescence In Situ Hybridization (FISH)

Fluorescence in situ hybridization (FISH) is a direct cell-based detection method. FISH combined with Epifluorescence microscopy (EFM), is generally accepted as a

cultivation-independent method to quantify microorganisms in the environment. [4] Over the past years, FISH has become a very strong tool in observing microbial communities in their environment. Epifluorescence microscopy (EFM) and flow cytometry are standard techniques for quantification of fluorescence-labeled microorganisms. However, FISH is a very time-consuming procedure in addition to being very costly. Although accurate, it is not a practical option. [11]

Rapid Diagnostic Test (RDT)

A practical alternative to the culturing method is using a Rapid diagnostic test (RDT). RDT is simple, easy to use and fast. The test kit can be stored without refrigeration and the cost is relatively cheap. The test procedure, excluding sample collection, requires 20–25 minutes. A widely used cholera RDT is based on the detection of an O-antigen: lipopolysaccharide (LPS). Developed by the Institute Pasteur, a French non-profit foundation dedicated to study of biological science, the RDT is a lateral flow immunochromatographic test for the qualitative determination of lipopolysaccharide antigen in 2 main serotypes of Vibrio Cholerae O1 and O139. The RDT is now being produced by Span Diagnostics (Surat, India) under the trade name Crystal VC™ at a price of 19.00 USD/test kit (10 test strips). The test kit is stable at temperatures between 4°C to 30°C, and test strips are packed in waterproof pouches, allowing storage under high humidity conditions.

Despite all the positive features, the accuracy of the diagnosis is only 54%. The user needs to distinguish between valid and non-valid test results, based on the appearance of one or two lines on the kit. The appearance of a very faint positive test line is often interpreted as a positive result, but could not be confirmed by culture. [10]

Biosensors and Lab on Chips

Bacteria culturing method, FISH and RDT are all based on biological and chemical properties of the Vibrio Cholerae bacterium. However, in the recent years the focus of engineers has turned to applications of biosensors and lab on chips.

The general function of all biosensors is to detect the presence of bacteria in a medium. The bacteria are manipulated by different methods to reach a detection system. Upon the detection of bacteria, a signal is transmitted and interpreted by the receiver. Biosensors can use chemical, optical, piezoelectric or electrical properties to determine the presence of bacteria in solid or liquid samples. Recent improvements in NEMS/MEMS technology has made it possible to achieve small and portable designs. A conventional sensor type is the electrochemical also referred to as impedimetric sensor. These sensors are designed to detect changes in impedance of the medium. Before getting into design details a rare characteristic of Vibrio Cholerae bacteria will be discussed in the next chapter.

CHAPTER 2

Vibrio Cholerae, A Magnetotactic Bacterium

Vibrio Cholerae is a 0.5x3 µm bacterium with a very long flagellum. In addition to having a long flagellum that makes mobility easier, Vibrio Cholerae is classified as a Magnetotactic bacterium. As shown in Figure 3, Magnetotactic bacteria (MTB) are motile bacteria that bio-mineralize a unique organelle called the magnetosome. Magnetosomes consist of a Nano-sized crystal of a magnetic iron mineral, usually either Magnetite (Fe3O4) or Greigite (Fe3S4), enveloped by a lipid bilayer membrane. In cells of almost all MTB, magnetisms are organized as a well-ordered chain. [12]

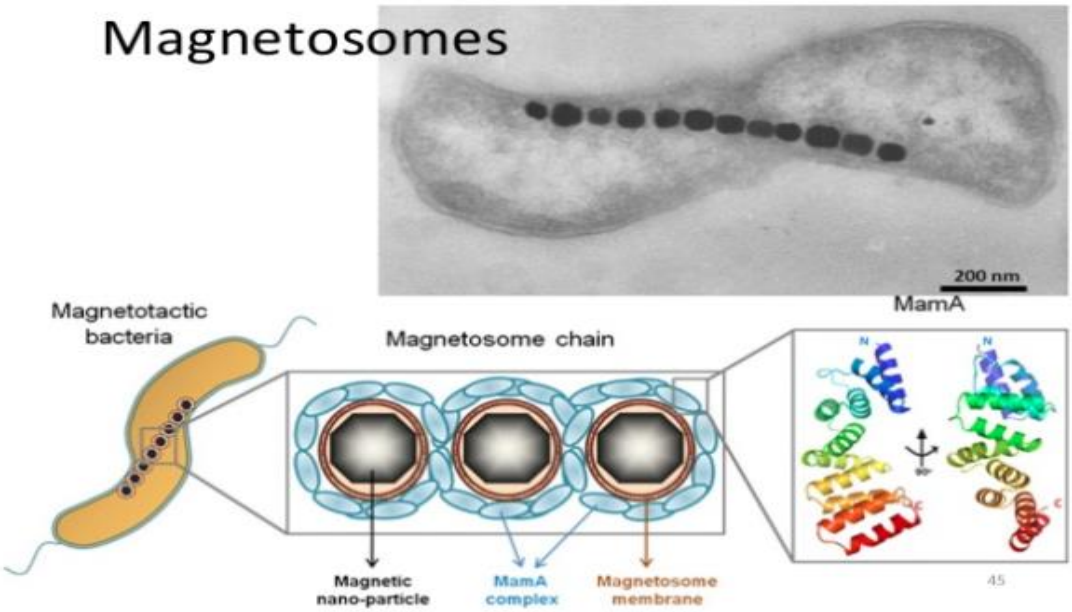

Figure 3:Magnetotactic bacteria and Magnetosomes [13]

The presence of Magnetosomes chain in Vibrio Cholerae gives the bacterium the ability to be motile, become a dipole in magnetic field and therefore be responsive to magnetic force and electric current. This rare feature has resulted in unique innovative designs for Magnetotactic bacteria detection devices.

An Innovative Detection System

A proposed design by Zhao Lu, Jaouad El-Fouladi from Ecole Polytechnique de Montréal, Canada is depicted in figure 4. It uses a different type of Magnetotactic bacteria, MC-1 to move immobile pathogenic bacteria to the detection microelectrodes. MC-1 responds to magnetic field and swims in direction of the field lines. The magnetic field direction can be controlled. MC-1 bacteria swim in average 100μ m/s. To capture the pathogenic bacteria, MC-1 bacteria are attached to conductive micro-beads coated with some specific antibodies. Bacteriophage specific to the targeted pathogenic bacteria is immobilized on the same bead. When the MC-1 bacteria swim in the sample and encounter a pathogenic bacterium, the bacteriophage should attack the latter and stick to it. Then, the magnetic field forces cause the MTB to go toward the sensing area where impedance measurement can begin. [14] The design can be applicable to different types of Magnetotactic bacteria such as Vibrio Cholerae.

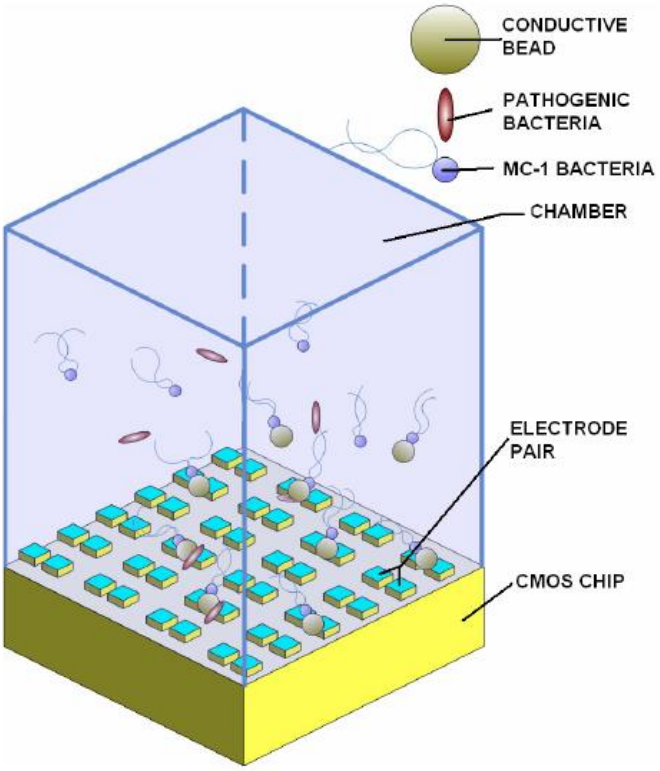

Figure 4:Proposed design by Ecole Polytechnique de Montreal, Canada [14]

Although the electrochemical sensors offer advantages such as high sensitivity and ease of integration onto a MEMS/NEMS device, long detection times (usually a 12-hour to 7-day process) are expected due to the long pre-amplification period if the initial concentration of bacteria is very low. Also in this case the coating of the microelectrodes needs to be Platinum or gold, which increases the cost significantly. [15]

The required signal processing is another challenge for impedimetric sensors. Due to the very small impedance signal, very precise and complex signal processing circuits are needed. There is also no complete design proposal for the required detection circuit in this proposed design.

In a second paper published by the same authors, a novel approach was proposed. It presents a CMOS based microfluidic/microelectronic hybrid microsystem for fast single

bacterium or micro-particle detection. The chip was designed using 0.18 μm CMOS technology. [15] The metal and via layers of CMOS were used to manufacture micro-channels between stacked pairs of microelectrodes. Figure 5 below shows a schematic of array of micro-channel and microelectrodes in the designed chamber with its two outlets.

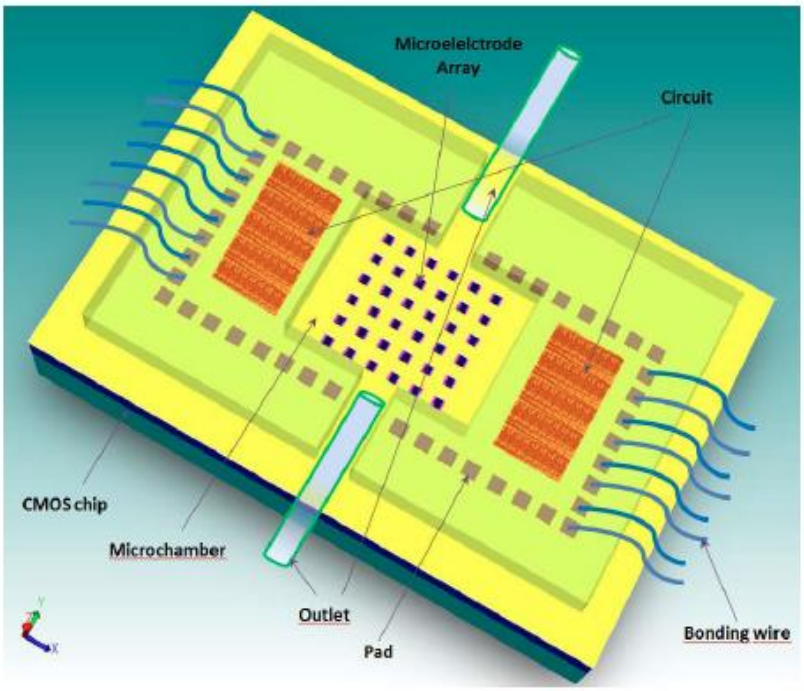

Figure 5: The chamber with the microelectrode arrays [15]

The liquid sample enters from one outlet while the other outlet is blocked. The sample will then distribute on the surface where micro-chambers are located. Due to pressure difference and gravity, the sample is guided to flow through the 8.05μm long micro-chambers. As shown in Figure 6 each micro-chamber has 5 pairs of microelectrodes stacked on top of each other. The inner layer of each micro-channel is coated with a thin layer of dielectric material (either Silicon oxide or Parylene) to isolate the microelectrodes from the sample liquid.

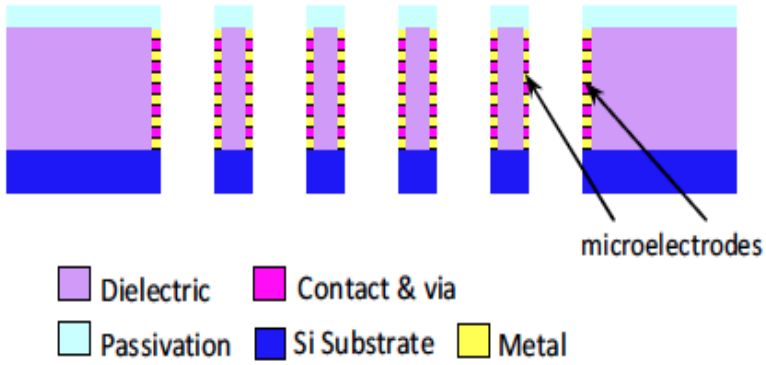

Figure 6: Stacked microelectrode pairs [15]

This configuration of microelectrode pairs can be modeled as two series capacitors, C_{OX}, separated by a series resistor, R_{SOL}, created as a result of the width of a micro-channel where the solution flows. As the bacteria or a coated micro-particle pass through the micro-channel, the value of this resistance changes. Monitoring this impedance change is key to detecting the presence of the bacteria. Each microelectrode pair is connected to a detection circuit.

Figure 7: Circuit model of an electrode pair [15]

The Prototype

The operating principle of the proposed detection circuit is shown in figure 8. In Operation a DC current I_{ref} is injected into the sample causing the voltage across the sample to increase.

(1) $V_{Rsol} = R_{sol} \cdot I_{REF}$

(2) $V_{C_{ox}} = \frac{1}{C_{ox}/_2} \int I_{REF}\ dt$

(3) $V_{sample} = V_{Rsol} + V_{C_{ox}} = R_{sol} \cdot I_{REF} + \frac{1}{C_{ox}/_2} \int I_{REF}\ dt$

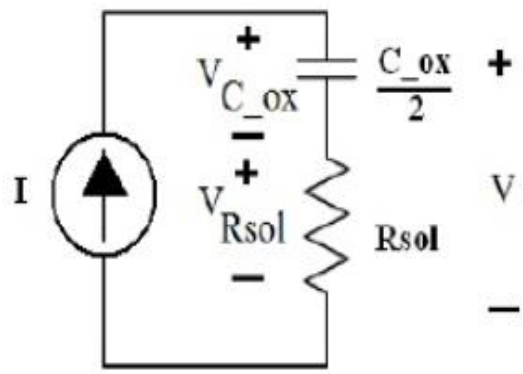

Figure 8: In operation a DC current Iref is injected into the sample causing the voltage across the sample to increase. The nature of the increase depends on the value of Rsol and thus the presence of bacteria.

The proposed conceptual detection circuit leveraging this basic operation is shown in figure 9.

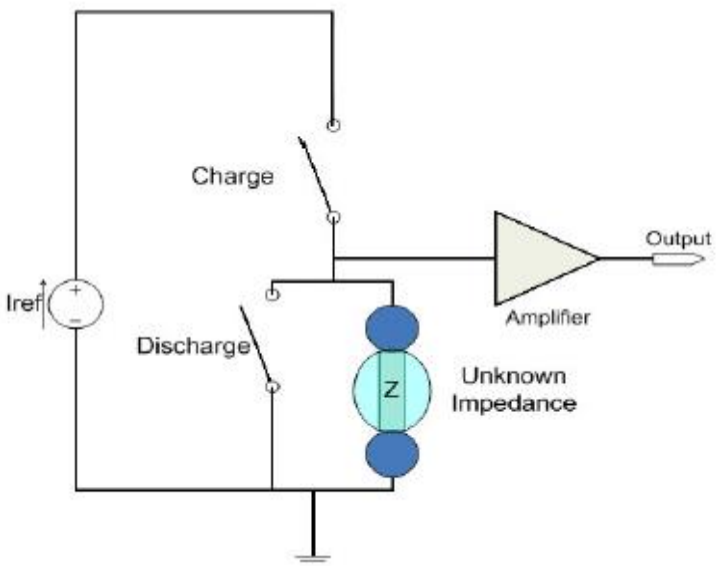

Figure 9: Diagram of detection system [15]

The switches are implemented using a PMOS and NMOS transistor, which are connected to a clock. When the charge switch is on and discharge switch is off, the constant current I_{ref} is lead to the upper microelectrode, charging the capacitors modeled by the sample and causing the voltage across the sample to increase. In operation the amplifier compares this voltage to a threshold. After some time, the charge switch is off, the discharge switch turns on. The input of the buffer is grounded. Both capacitors will discharge gradually. After a suitable time, the process is repeated. The result is a pulse train created at the output of the amplifier. The widths of the created pulses are related to the value of impedance of the solution. The pulse becomes wider as higher impedance is detected. The generated pulses with varied impedances are shown in figure 10.

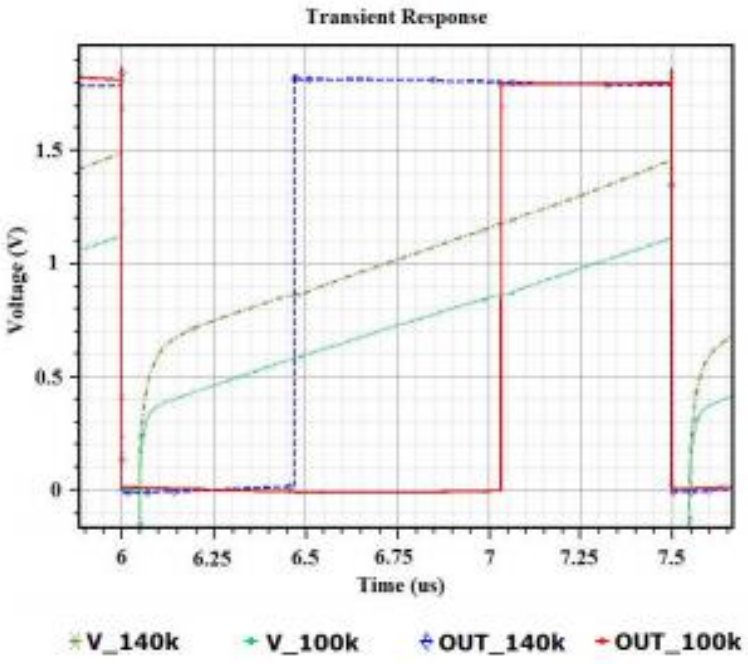

Figure 10: V_140K and V_100K show the input to the amplifier and corresponding outputs for different values of Rsol [15]

Therefore, an automatic system can analyze the pulse width and determine if bacteria are present or not.

Advantages

The design from Ecole Polytechnique de Montréal, Canada's team uses an inherited genetic property of the deadly bacteria, which can be manipulated using basic electronics and physics laws. This design could lead to a very fast, efficient and portable device to detect Vibrio Cholerae Bacteria and to potentially save thousands of lives.

Shortcomings

Although the proposed design in [15] is promising, it is not complete. The microelectrode arrays were fabricated but never implemented in a complete system on a chip. The system requires external laboratory equipment to function. The resulting system is costly, complex, bulky and power hungry, thus, precluding widespread use in developing countries. Another issue is the lack of a simple output that determines the existence of the bacteria.

The design discussed in following chapter extends that of Zhao Lu and Jaouad El-Fouladi's by integrating necessary support electronics onto the same chip as the sensor itself for a low cost, low power, highly miniaturized lab system-on-a chip in this way moving this technology closer to practical third world use.

CHAPTER 3

Bacteria Detection Platform

The hybrid bacteria and microparticle detection platform on a CMOS chip designed by the engineering team at Ecole Polytechnique de Montréal offers an innovative approach to CMOS biosensors. However, the system needs to be functional.

This thesis offers a complete, fast, efficient and low power CMOS sensor platform based on 500 nm, 3.3v technology of On-Semi process for detection of Vibrio Cholerae bacteria. The following block diagram depicts the flow of the proposed system.

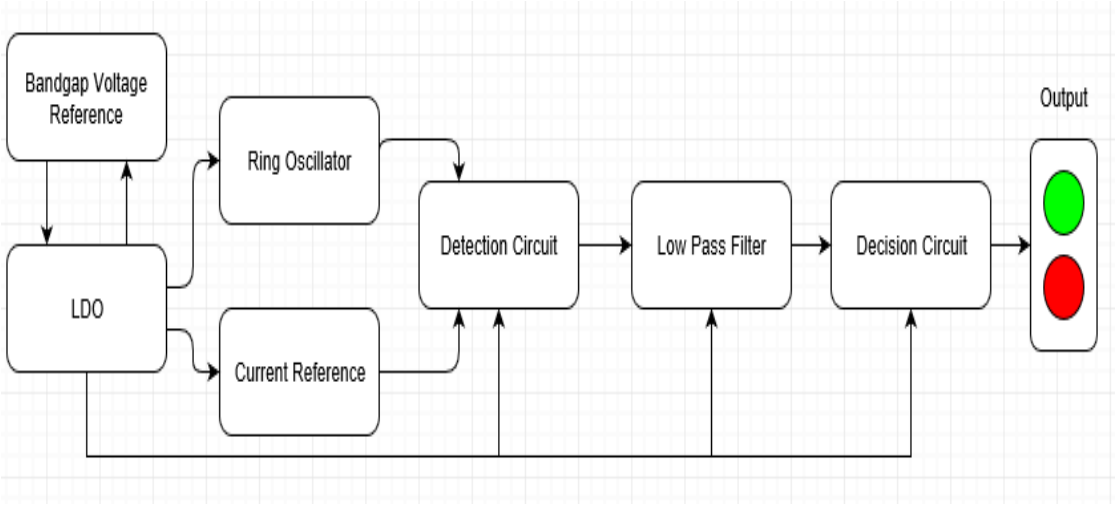

Figure 11: Block Diagram of designed bacteria detection system

A voltage bandgap reference is designed to supply a steady input power across a wide temperature range- this might be helpful for third word use. A low-dropout regulator LDO will maintain a constant input voltage to all parts of the system. The design includes a temperature independent current source to activate the detection circuit. This self-biasing current source is immune to changes of the supply voltage. In addition to a current source, the detection circuit needs a ring oscillator to work as a clock signal for its switches. The output signal of the detection system is filtered and amplified through a

low-pass filter to create a square wave output signal. The output signal is then run through a decision circuit where it is interpreted as a simple, binary LED light output that indicates the presence or the absence of the bacterium in the tested sample.

The Detection Circuit Components

Current Reference

The detection circuit needs a current source. A thermal voltage based current reference was selected for its insensitivity to temperature and power supply fluctuations.

The design is shown in figure 12 below:

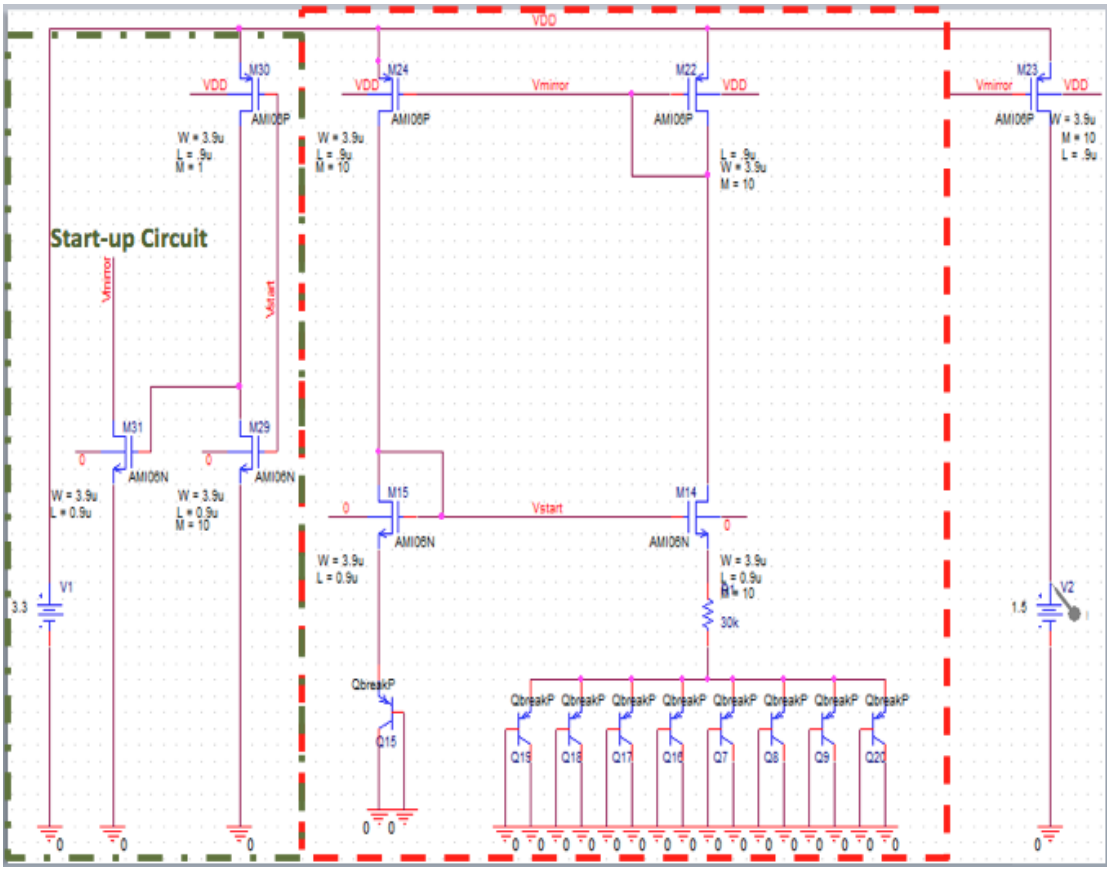

Figure 12: Current reference schematic

The configuration of the current mirror used in the current reference design is shown confined in the red dashed box in figure 12.

For the current to be independent of the supply voltage and its fluctuations, bootstrap bias technique can be used. A circuit using this method biases itself; hence the circuit of choice has a “self-biasing” topology. Instead of developing the input current by

connecting a resistor to the supply, the input current is made to depend directly on the output current of the current source itself [17]. The block diagram in figure 13, depicts the relationship of the input and output currents of the system.

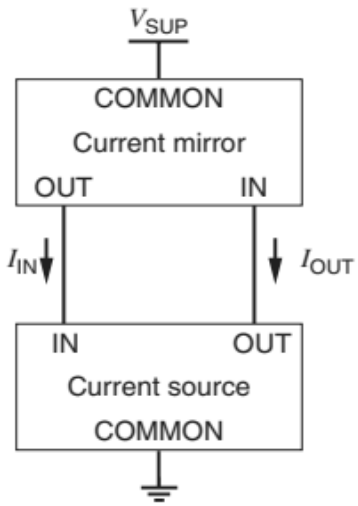

Figure 13: Input and Output currents block diagram

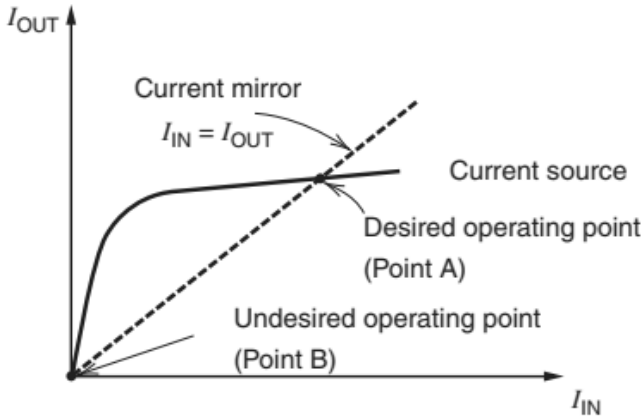

Figure 14: Changes in output current relative to change in input current

From the standpoint of the current source, the output current is almost independent of the input current.

Changes in the output current over a wide range of input currents, is shown in figure 14. From the standpoint of the current mirror, I_{IN} is set equal to I_{OUT}, assuming the gain of

the current mirror is unity. There are two potential operating points for this circuit. Both are shown in the plot of figure 14. Point A is the desired operating point, and point B is an undesired operating point because $I_{OUT} = I_{IN} = 0$. [17]

At point B, all the transistors are not conducting. It is necessary to implement a start-up circuit to prevent the current reference circuit from operating in the undesired zero-current state.

Start-up Circuit:

A startup circuit is used to ensure the self-biasing current reference starts and stays in the desired operating point and has a very small leakage current when off. The configuration highlighted within a dashed green box in Figure 12, shows a start-up circuit made from a common source implementation of an NMOS transistor M_{31} connected to an inverter. In the "zero-current" operation state, all four transistors M_{14}, M_{15},M_{22} and M_{24} are not conducting. As a result, equation 4 is valid for the voltage on the connecting branch between the gates of the PMOS transistors, marked with V_{mirror}.

(4) $V_{mirror} = V_{dd}$

Also on the connecting branch of the two NMOS transistors:

(5) $V_{start} = 0$

The equation above, makes the output of the inverter to be 1 (high), turning on transistor M_{31}. The M_{31}transistor operates as a switch and once on, pulls V_{mirror}down.

As V_{mirror} changes, the gate voltage on M_{22} and $M_{24}$is affected, current starts flowing in the devices and moves to the operating point to the desired one. At that point the start-up circuit is turned off and has a very small leakage current. This start-up circuit ensures that the current reference circuit never operates in the undesired zero-current state.

Another important aspect of this current reference design is to make the current reference to be immune to temperature fluctuations.

An important aspect of the performance of a current reference is its fractional temperature coefficient (TC_F). TC_F is expressed as the change in the output current with respect to the temperature fluctuations. To design a temperature independent system (zero temperature coefficient) proper weighing of two components with opposite temperature coefficient signs is required.

To achieve this goal, as shown in figure 12, the collector and base terminals of each BJT transistor are grounded. The emitter-base junction of the NPN transistor therefore behaves similar to a diode. If two bipolar transistors operate in unequal current densities, the difference in their base-emitter voltages is proportional to absolute temperature. Implementation of 8 transistors on one branch vs. 1 on the other results in unequal current densities.

The thermal voltage V_T is another temperature dependent parameter. The transistors on the two branches operate in different current densities ($I_{S_{Left}}$ and $I_{S_{Right}}$). If the ratio of the input to the output current is held constant, the voltage across the 30Ω resistor is proportional to the thermal voltage V_T. Considering n as the ratio of BJT transistors on the left vs. right side ($n = 8$) and

(6) $$V_T = \frac{kT}{q}$$

Then,

(7) $$I_{Out}R = \left|V_{BE_{Left}}\right| - \left|V_{BE_{Right}}\right|$$

$$= \frac{kT}{q} ln(\frac{I_{IN}}{I_{S_{Left}}}) - \frac{kT}{q} ln(\frac{I_{Out}}{I_{S_{Right}}})$$

$$= \frac{kT}{q} ln(\frac{I_{IN}}{I_{S_{Left}}} \frac{I_{S_{Right}}}{I_{Out}})$$

(8) $$I_{Out}R = \frac{kT}{q} ln(n)$$

The output current of the current reference circuit can therefore be expressed with:

(9) $$I_{Out} = \frac{1}{R} \frac{kT}{q} ln(n)$$

The variation of I_{Out}vs. Temperature:

(10) $$\frac{\partial I_{Out}}{\partial T} = ln(n) \frac{R\frac{\partial V_T}{\partial T} - V_T \frac{\partial R}{\partial T}}{R^2}$$

$$= ln(n) \frac{V_T}{R} (\frac{1}{V_T} \frac{\partial V_T}{\partial T} - \frac{1}{R} \frac{\partial R}{\partial T})$$

As a result, the temperature coefficient TC_F:

(11) $$TC_F = \frac{1}{V_T} \frac{\partial V_T}{\partial T} - \frac{1}{R} \frac{\partial R}{\partial T} = \frac{1}{T} - \frac{1}{R} \frac{\partial R}{\partial T}$$

TC_F of resistor was modeled as a polysilicon resistor with a typical value of 1000E-6 ppm.

TC_F of resistor and $\frac{kT}{q}$ partially cancel! [17]

The plot on figure 15, shows the temperature coefficient of the design system vs. on a range of temperature.

The current variation of the output current as the temperature changes from 0℃ to 100℃ is only 2nA.

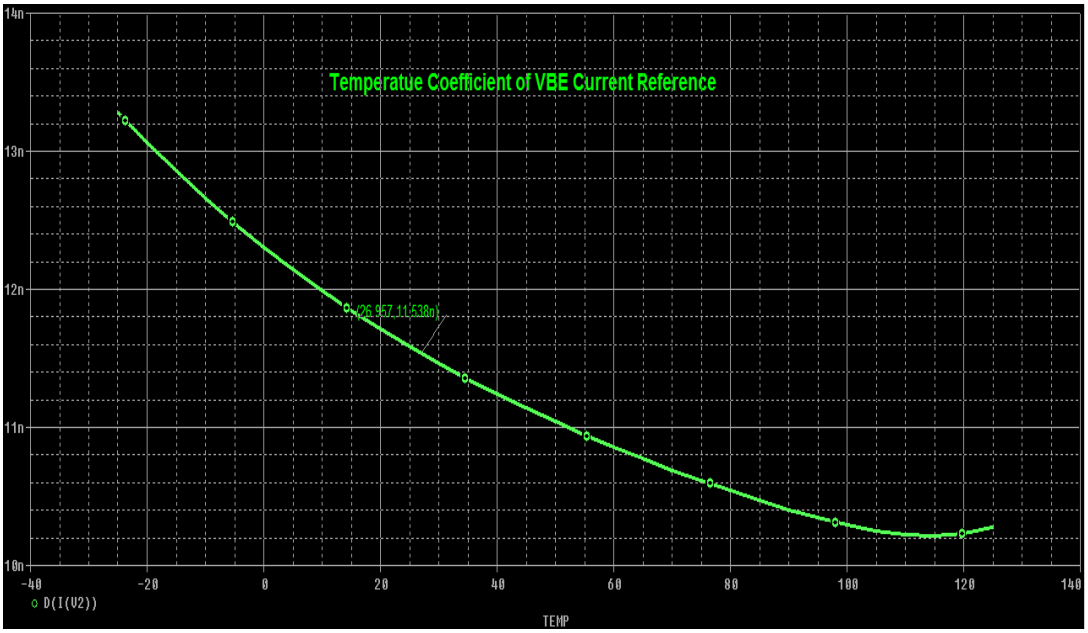

Figure 15: Temperature coefficient of VBE current reference

The final step in the current reference circuit is to copy the output current. The voltage compliance of this final step is depicted in figure 16:

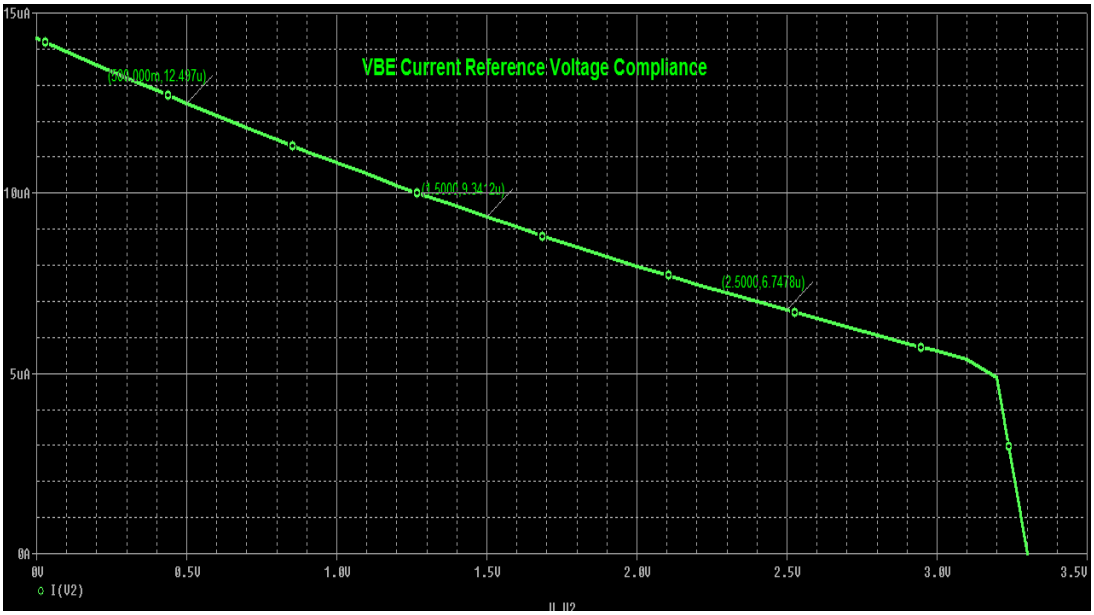

Figure 16: VBE Current reference's voltage compliance

Bandgap Voltage Reference

The objective is to design a system with a controlled temperature dependence, which establishes a stable and precise dc voltage that is independent of the supply voltage V_{dd} fluctuation with a low voltage drift over temperature. Temperature independence of the voltage reference reduces its process dependence.

As explained previously the thermal voltage based current source designed for this system is very immune to temperature and supply voltage variations. As shown in figure 17, placing diode connected BJT transistor at the output branch of the designed current source provides a voltage reference, which is immune to temperature variations.

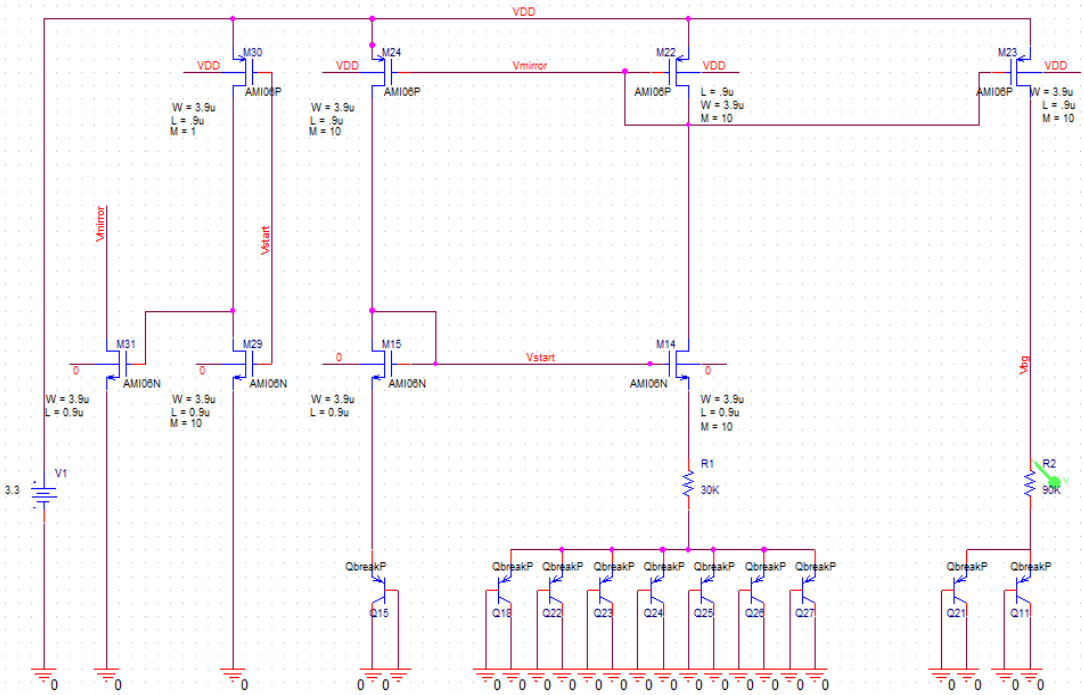

Figure 17: Bandgap voltage reference schematic

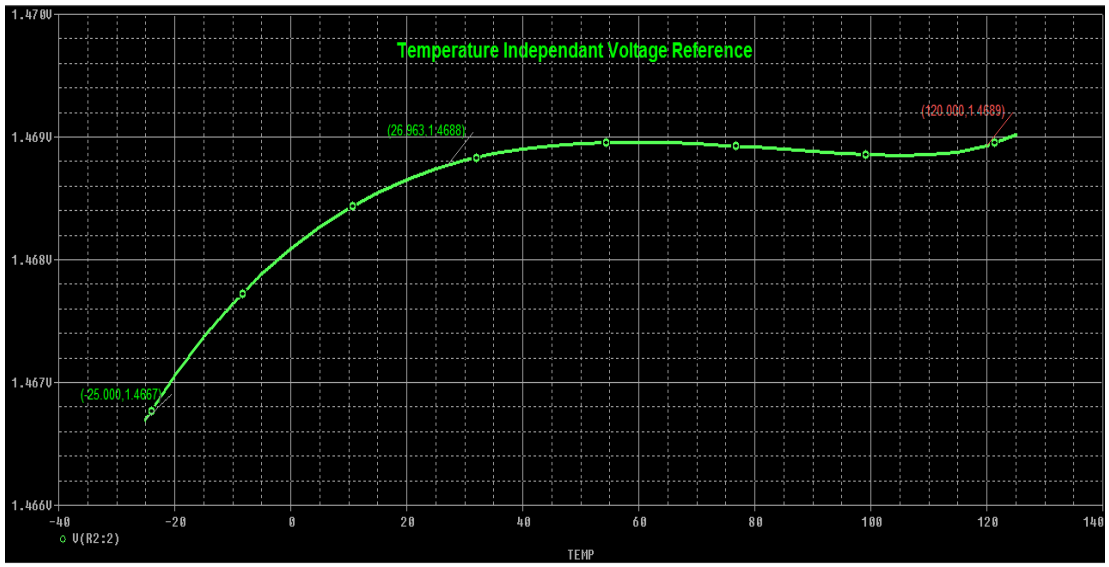

Figure 18: Temperature independent voltage reference

To design an effective voltage bandgap reference, there are numerous important parameters to be considered including temperature drift, power supply rejection, thermal hysteresis, power consumption.

Temperature Drift

Providing a precise and stable voltage over temperature is an essential part of an accurate design. Temperature coefficient (TC) refers to the drift of the output voltage of the system over temperature. Considering V as the voltage reference output, TC at room temperature (25°C) is calculated in parts per million over degree Celsius by:

(12) $$TC_0 = (\frac{1}{V}) \times \frac{dV}{dT} \times 10^{-6}\ [ppm, °C]$$

The temperature coefficient of the bandgap voltage designed can be observed in figure 19:

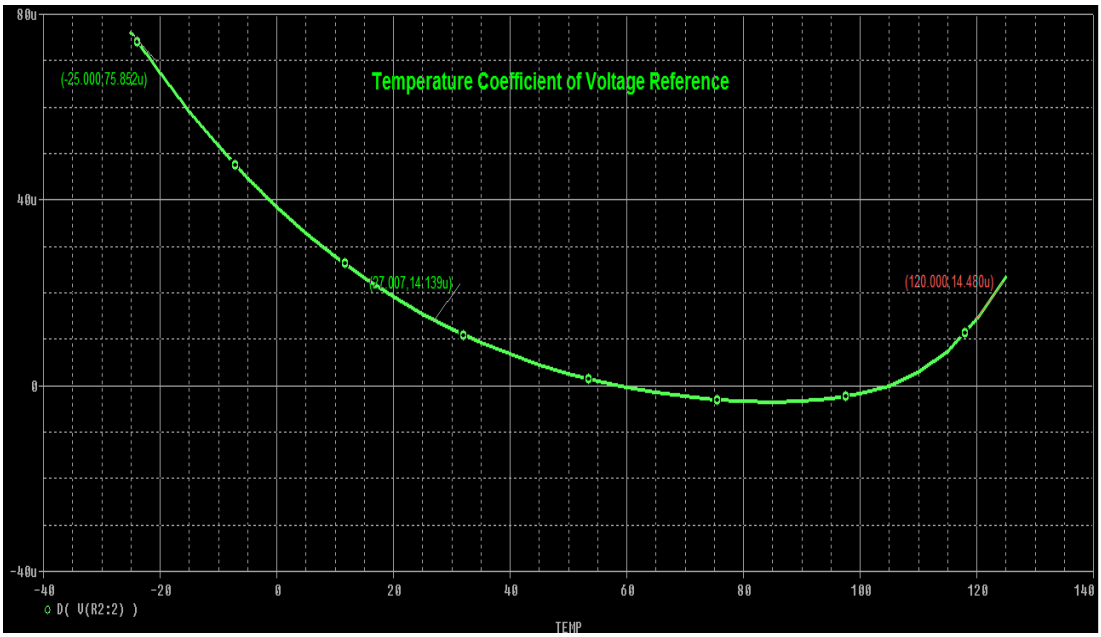

Figure 19: Temperature coefficient of voltage reference

Power Supply Rejection (PSR)

The ability of the voltage reference to resist the noise and unwanted signals provided by the power supply is measured by Power supply rejection (PSR). PSR is defined in decibels. It expresses the tolerance of the system toward noise at a certain frequency, and it's used to predict the system's voltage variation behavior over a range of frequencies.

(13) $$PSR_f = 20\ log\ \frac{V_{ref}}{V_{Supply}}$$

Where V_{ref} is the voltage reference's output and V_{supply} is the supply's voltage at frequency *f*.

Thermal Hysteresis

Thermal hysteresis is a phenomenon where the system is not only dependent on its temperature but also its thermal history. Sometimes the output voltage of the voltage reference drifts from its original value after a temperature cycle. If the room temperature is referred to as the base temperature, this phenomenon can be described by the equation below.

(14) $$V_{ref-hyst} = \frac{V_{ref-25°C} - V_{ref-Cycle}}{V_o}$$

Where $V_{ref-25°C}$ is the output voltage at room temperature.

$V_{ref-Cycle}$ is the output voltage after a temperature cycle.

V_o is the expected constant output voltage.

LDO: Low Dropout Voltage Regulator

Low dropout regulator (LDO) is designed to regulate and stabilize an output voltage provided by a higher input voltage. An LDO's application in this platform is to provide the system's required 3.3v voltage from batteries with any value more than 5 volts. This feature is designed for the user's convenience in addition to its benefits in circuit's performance.

There are two types of linear regulators: standard linear regulator and low dropout linear regulators (LDOs). The difference between the two is in the pass element and the amount of headroom, or dropout voltage, required to maintain a regulated output voltage. The dropout voltage is the minimum voltage required across the regulator to maintain regulation. The input voltage minus the voltage drop across the pass element equals the output voltage. For standard regulators the pass element is usually a Darlington NPN or PNP. [18] The voltage drop across collector to emitter is high because as shown in figure 20, the drop occurs twice on base-emitter junction before reaching the output.

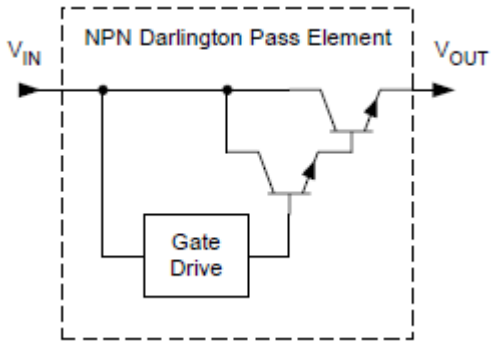

Figure 20: NPN Darlington pass element

LDO requires much lower dropout voltage. A block diagram of the designed LDO for detection system's application is depicted in block diagram shown in figure 21.

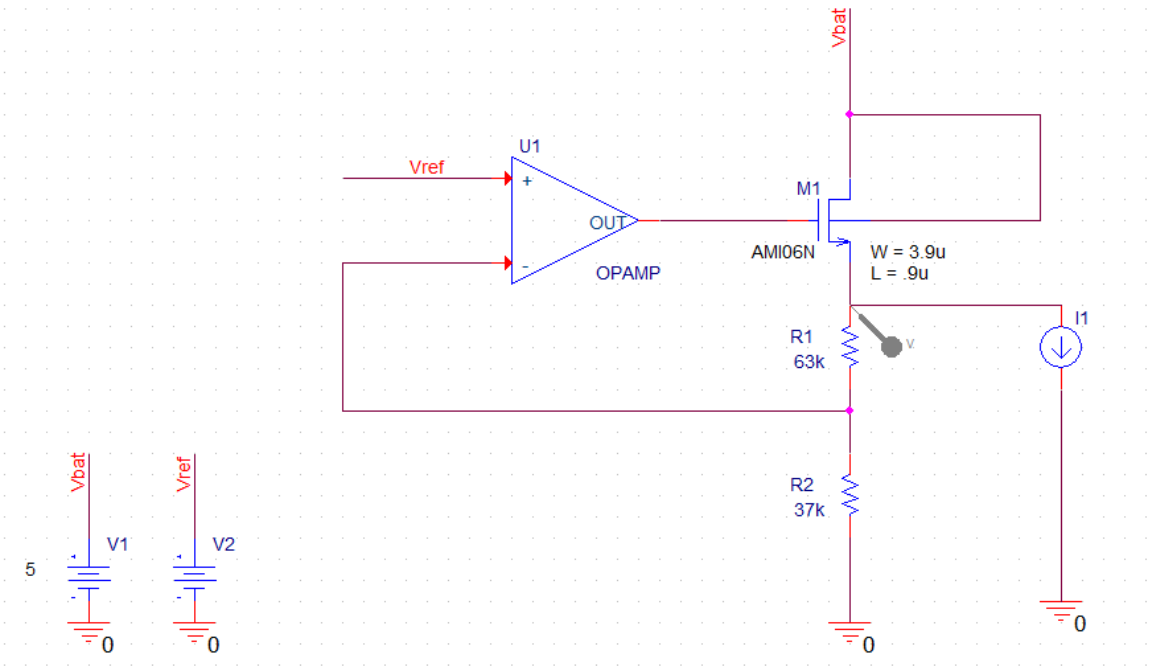

Figure 21: LDO's Diagram

The input voltage is applied to a pass element, an N-channel FET, which operates in the linear region to drop the input voltage down to the desired output voltage. The resulting output voltage is sensed by the amplifier, and it is compared to the reference voltage. The amplifier drives the pass element's gate to the appropriate operating point to ensure that the output is at the correct voltage. As the operating current or input voltage changes, the amplifier modulates the pass element to maintain a constant output voltage. Under steady state operating conditions an LDO behaves like a resistor however since the operation conditions are never static, the feedback is necessary to change the LDO's effective resistance to maintain the output voltage. [18] An example of LDO's voltage regulation is when the load resistance decreases i.e. the current increases. The LDO must decrease the pass element's resistance by increasing the gate to source voltage on the NMOS. When

the gate to source voltage increases, the operating mode moves upward assuming a fixed input and output voltage.

LDOs enter dropout region at about:

(15) $V_{IN} - V_{OUT} = 0.4v$

An LDO's output noise is reduced when it is near or in this operating region. All bandgap references produce noise and it is fed directly to the amplifier. The noise on the output of the amplifier modulates the pass element's gate voltage creating noise on the LDO's output. When an LDO is in dropout, the amplifier's output is at its maximum, which reduces its ability to pass bandgap noise from its input to its output. [18]

Figure 22, shows the LDO designed including the amplifier and the pass element used.

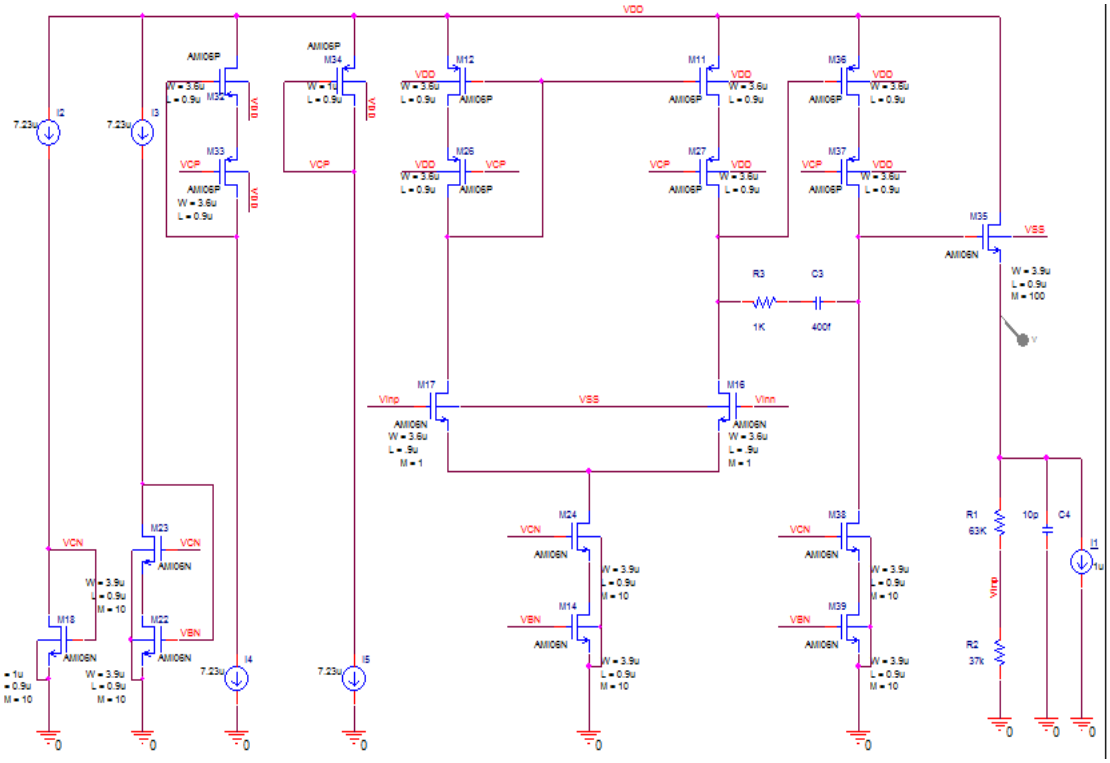

Figure 22: LDO's schematic

The Bode plots shown in figure 23, show the gain and phase margin of the designed amplifier. Phase margin is simulated to be 46°. Stability of LDO's feedback system is therefore ensured.

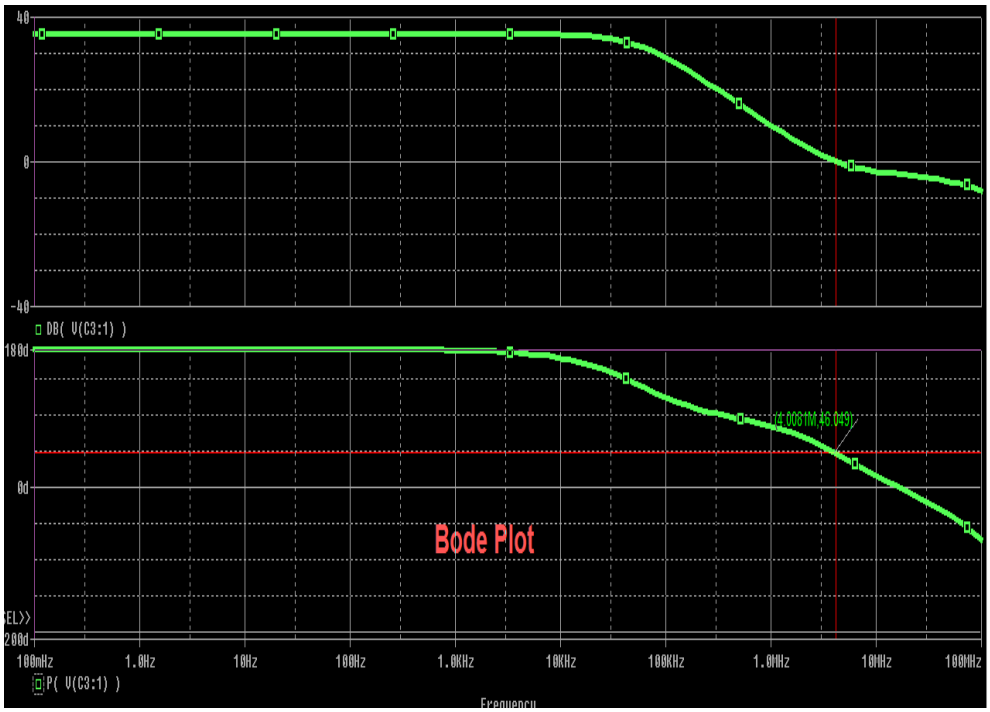

Figure 23: LDO's gain and phase margin Bode plots

As depicted in figure 24, the LDO will maintain a 3.3v voltage across the whole circuit, regardless of the changes in the supply voltages of 5v or more.

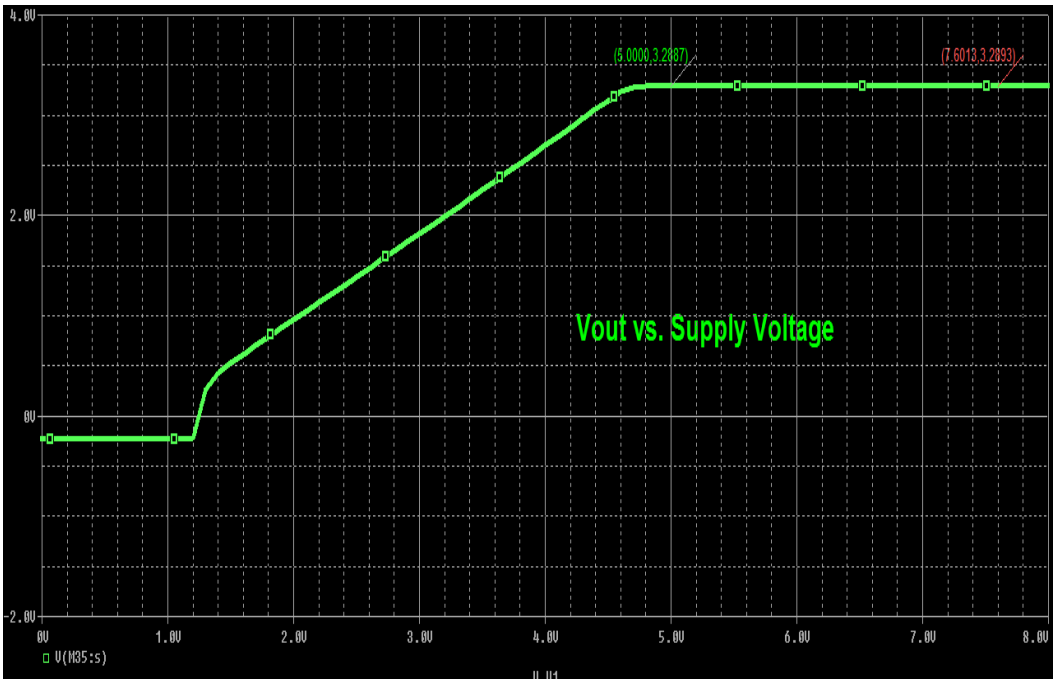

Figure 24: LDO's Vout vs. Supply voltage

Ring Oscillator

A ring oscillator is a combination of odd numbers of inverters. A single CMOS inverter circuit and its digital symbol are shown in figure 25 and 26 below. The goal of an inverter is to provide digital logic 0 or 1 output. Provided with low state ”0“ input, the inverter outputs a high state “1” output and vice versa. CMOS inverter can be implemented using a PMOS and a NMOS transistor.

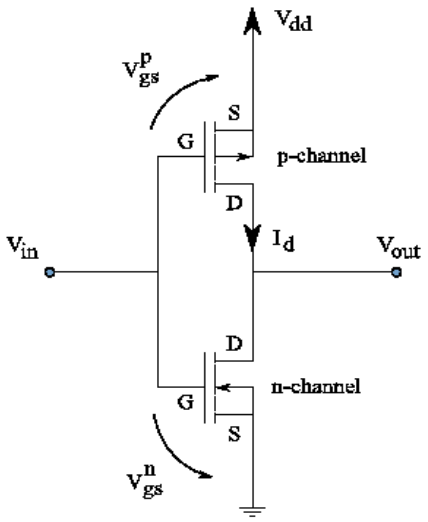

Figure 25: CMOS inverter

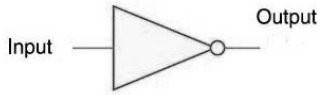

Figure 26: Inverter symbol

Both gates of the PMOS and NMOS transistors are connected to V_{in}. This arrangement puts the transistors in complementary states. Once V_{in} is high, close to the value of V_{dd}, the voltage on the gate of NMOS transistor causes it to be on; but it has an opposite effect on PMOS transistor, turning it off. The output voltage is therefore pulled to the ground (low). If V_{in} is low, then NMOS is off and PMOS is on. The output voltage is pulled to

high state (V_{dd}). To implement a ring oscillator, an odd number of CMOS inverters are put in series. Connecting the output to the input of the next. The last output is connected to the first input. This configuration causes the last output to oscillate between a high and low state.

The complete schematic of the ring oscillator used in this detection system is shown in the following figure:

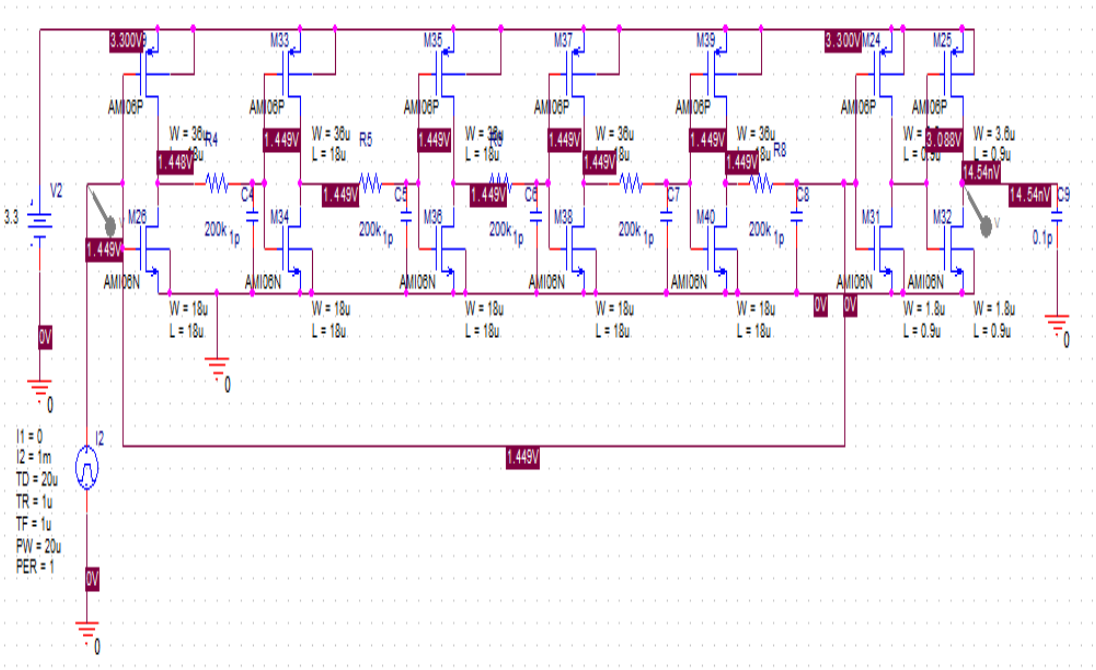

Figure 27: Ring oscillator schematic

For this detection circuit, 5 inverters were used to design a ring oscillator operating as a clock for the switches on the detection circuit. The period of the pulse is thus designed to provide sufficient time for charging and discharging of the capacitor C_5 in figure 29. To optimize the design, the PMOS transistors' sizes were set to W=36 μm and L=18 μm and NMOS transistors to 18 μm for both width and length. A 200kΩ resistor and a 1pF Capacitor were placed after the output of each inverter to create the desired delay to

increase reach a period of 10 μs. Two additional inverters were placed at the final output of the ring oscillator to create a perfect square output wave. The following figure 28, is the simulation results. The Blue signal depicts the input pulse to the ring oscillator, and the red output signal shown the resulting desired smooth square wave.

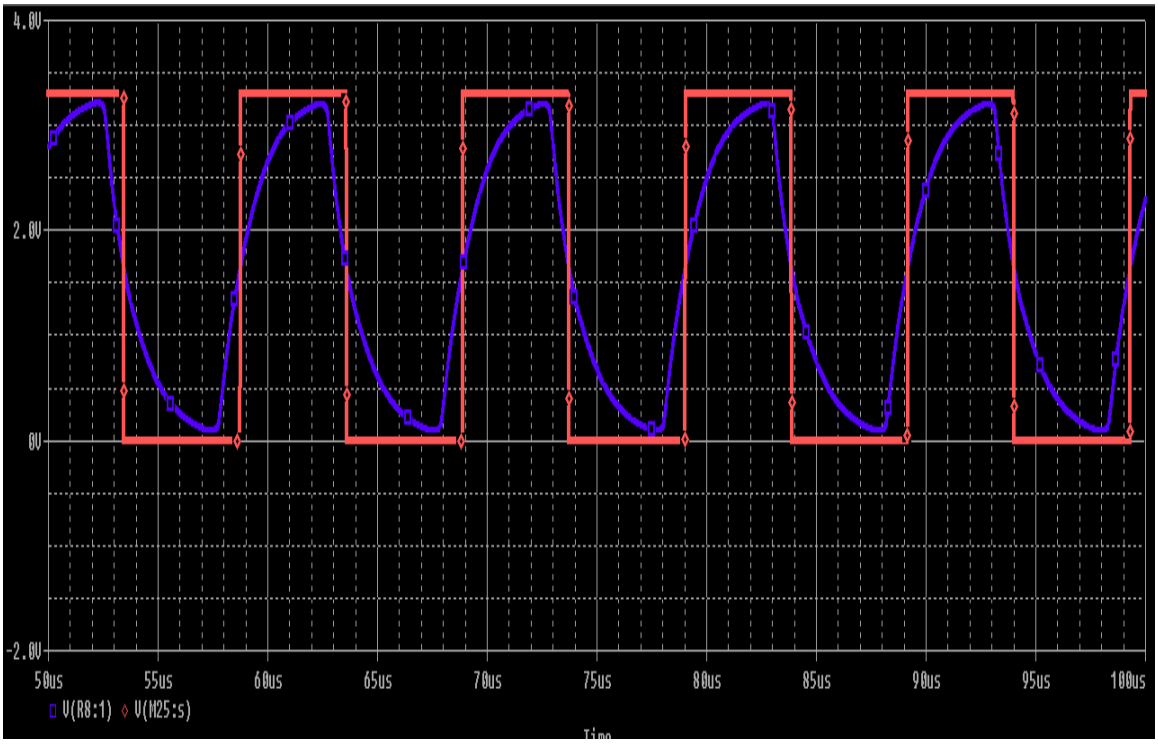

Figure 28: Input and output signals of the ring oscillator

Detection Circuit

The detection circuit is implemented based on the proposed design from the hybrid bacteria and microparticle detection platform on a CMOS chip paper by the engineering team at Ecole Polytechnique de Montréal.

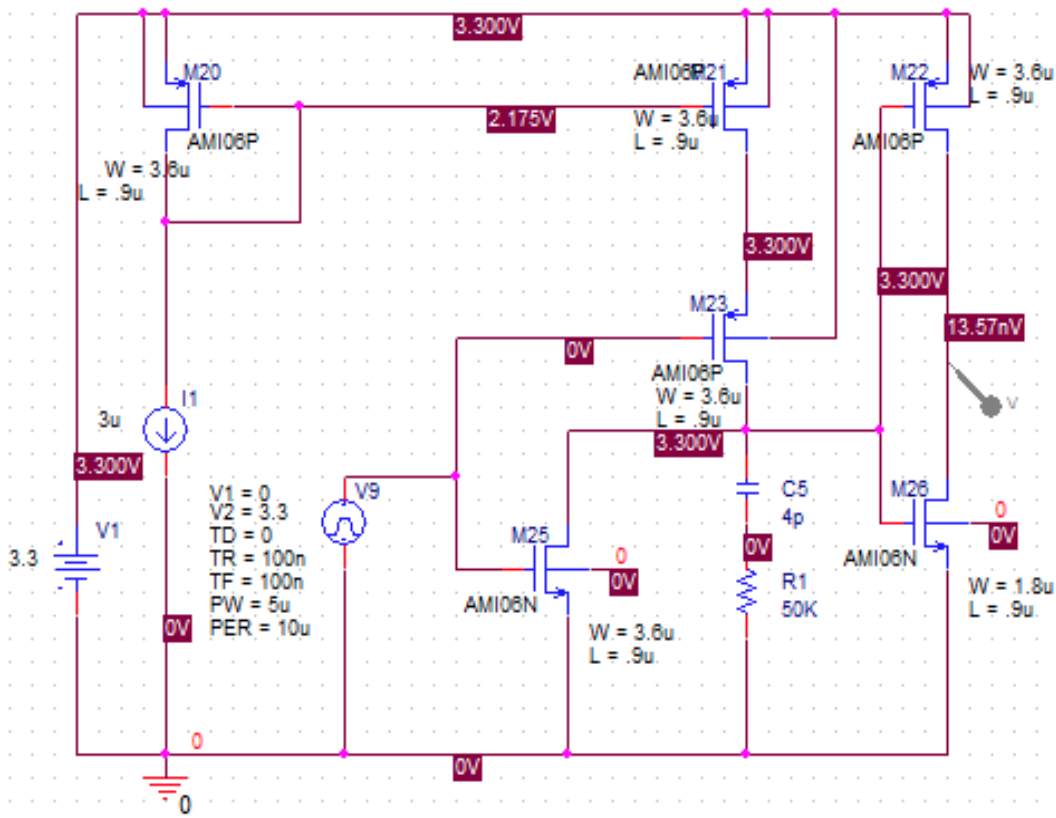

Figure 29: The main detection circuit

The configuration of a microelectrode pair is shown in figure 6. The created capacitance C_{ox}due to the width of a micro-channel, and the solution's resistance R_{sol} are modeled with capacitor C_5 and Resistor R_1. The experimental value for each micro-channel capacitance is between 5 to 8 pF. Experimental tests show that if a magnetic microbead modeling the Cholera bacteria contaminated solution flows through the channel, the resistance R_1 is changed from 50kΩ to 400$k\Omega$. The difference between presence of

bacterium vs. its absence is marked as before and after. The bandgap voltage reference and the LDO described previously provide a steady 3.3v to power up the circuit. The output signal of the ring oscillator is modeled as V_9 source which pulses act as a clock signal. Based on V_9 being high or low, only one of the two transistors $M_{23}$and M_{25}will be on. While $M_{23}$is on and $M_{25}$is off, the current I_1 provided by the temperature independent current source, charges capacitor C_5. As M_{23}turns off and M_{25} turns on, C_5 is discharged. The continuous nature of the clock signal, creates periodic pulses which show the change in impedance of a microelectrode pair. Changes in resistance affects the width of the pulse because the time constant τ is defined by:

(16) $\tau = RC$

The two detection circuits shown in figure 30, are used to simulate and to demonstrate this impedance change, under two conditions. First circuit has 50kΩ as it is designed to show the circuit's performance where no bacteria are detected in the micro-electrode pair. The second circuit on the right however is designed with a 400kΩ resistance to simulate the presence of bacteria.

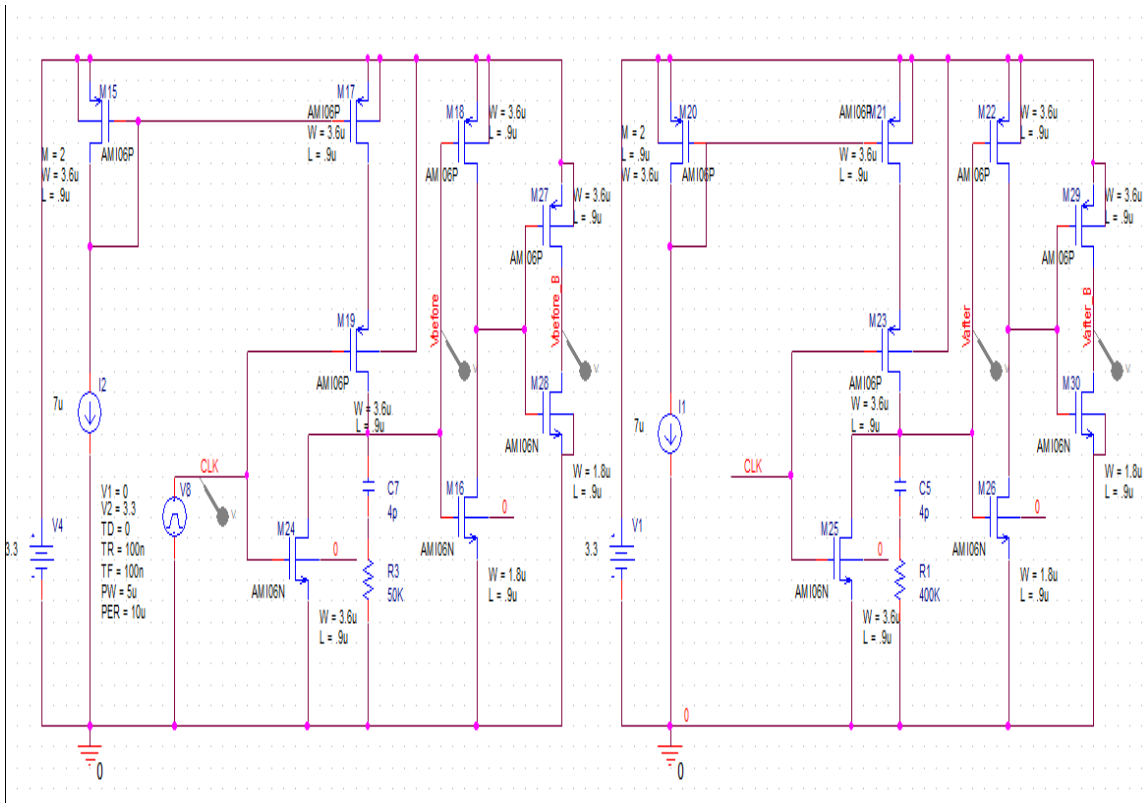

Figure 30: Detection circuit schematic with 2 different detected resistances

In the following graphs the green plot shows the simulation result when R=50kΩ which is compared to the red plot demonstrating R=400kΩ.

The effect of change in the time constant τ is very evident in the top graph. The larger the resistance value, the larger the time constant.

As shown in schematic in figure 30, the signal passes through an inverter as the last step. The inverter's effect on the signal shown in the top graph in figure 31 is depicted in the bottom plot where the width of the pulse corresponds to the switching threshold of the inverter. The pulse width is 5μs when bacteria are present, compared to 3.5μs in its absence.

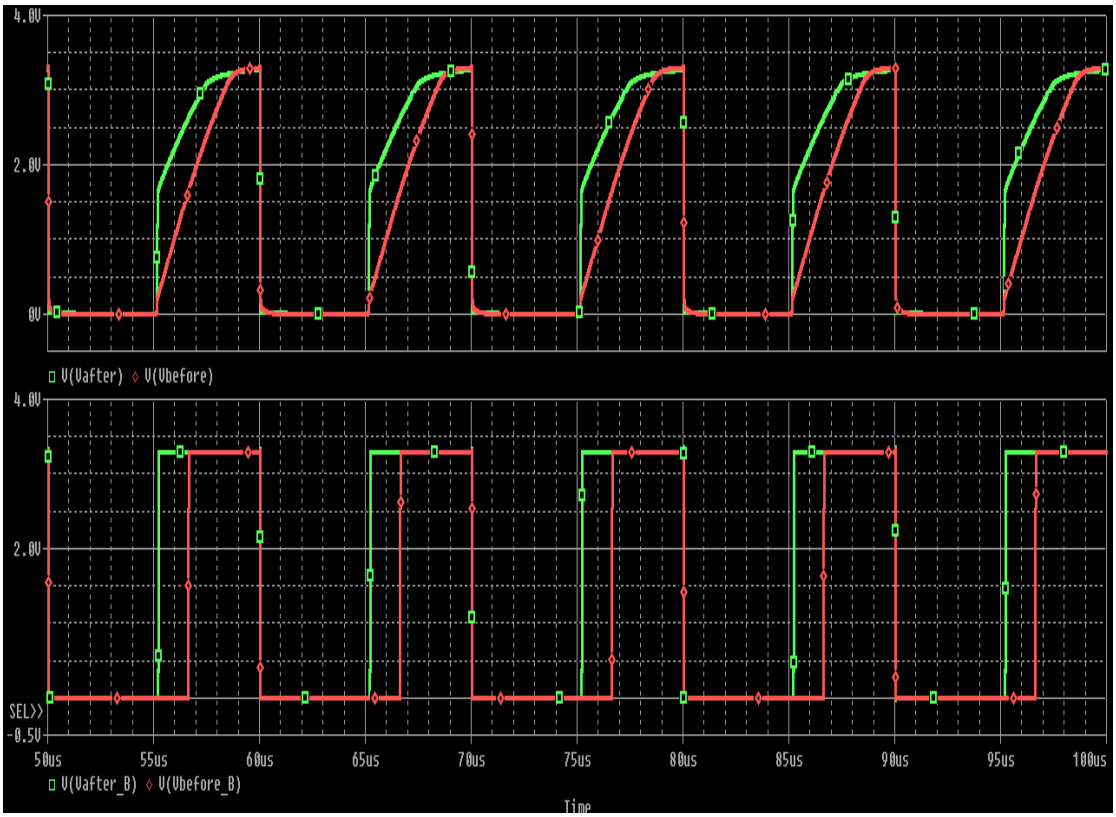

Figure 31: Detection output with and without the inverter

Two-Stage Operational Amplifier

The two-stage operational transconductance amplifier (OTA) is a building block for many analog circuits.

A two-stage op-amp configuration isolates the gain and swing requirements. The first stage provides high gain while the second stage gives large swings. In designing an OTA there are several critical parameters to be considered. Noise, phase margin, gain-bandwidth product, load capacitance, slew rate, input common mode range (CMR) and output swing some to be named. Other parameters such as dc gain and CMRR are dependent on the output resistance of the MOSFETs. The schematic of the designed operational amplifier is shown in figure 32.

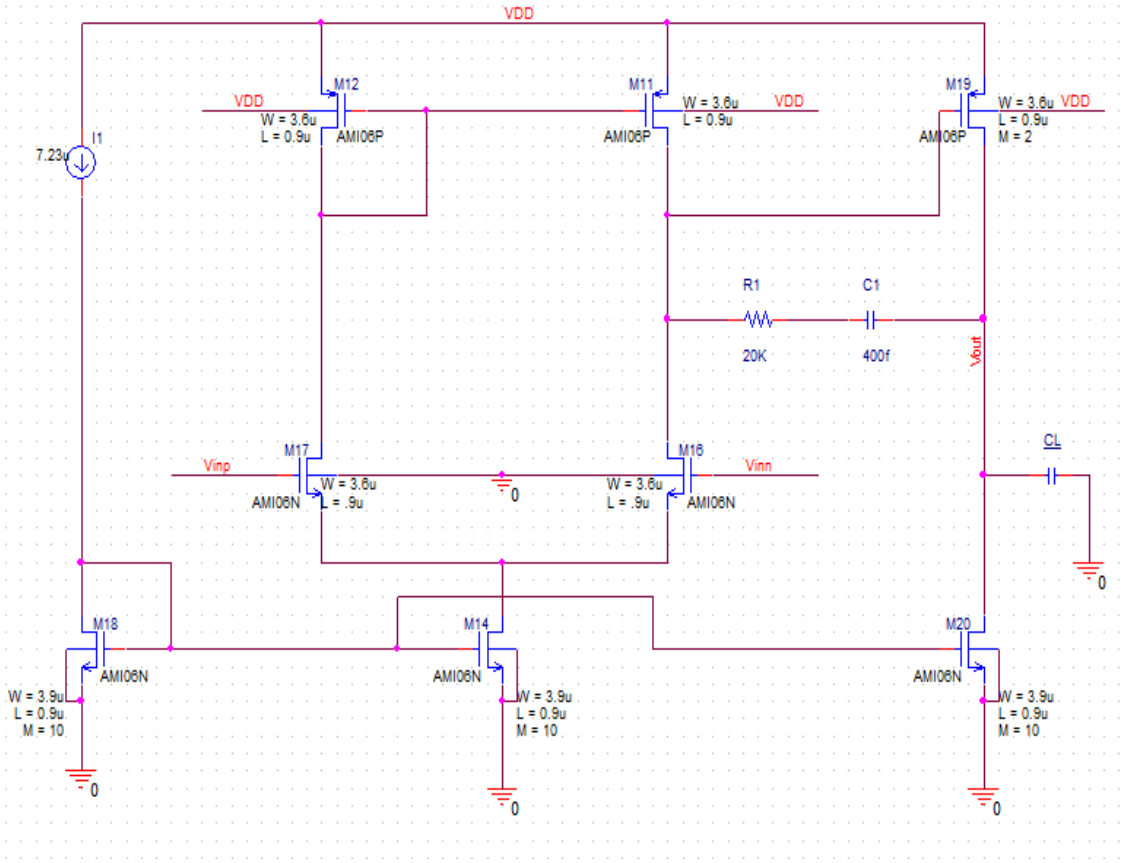

Figure 32: Operational amplifier's schematic

In this design, the Miller compensation and the nulling resistor is used to compensate for the right half-plane zero. The transconductance gain of transistors $M_{17}$and $M_{26}$is calculated using the input noise voltage spectral density formula.

(17) $S_n(f) = 2 \times 4kT \times \frac{2}{3} \times \frac{1}{g_{m17,16}}[1 + \frac{g_{m12,11}}{g_{m16,17}}]$

(18) $g_{m16,17} = \frac{16}{3} \times \frac{kT}{S_n(f)}$

The flicker noise is ignored in the equations above however it can be controlled by changing the proportions of $M_{16}$and M_{17} transistors.

the compensation capacitor can also be calculated by:

(19) $C_1 = \frac{1}{2\pi}\frac{g_{m16,17}}{f_{GBW}}$

Both slew rates of the output of the differential stage and the output of the two stage OTA are related to quiescent currents:

(20) $SR_1 = \frac{2I_{D16,17}}{C_1}$

(21) $SR_{output} = \frac{I_{D_{20}} - 2I_{D16,17}}{C_L}$

Setting both slew rates equal:

(22) $SR_1 = SR_{output} = SR$

(23) $I_{D16,17} = \frac{SR}{2} \times C_1$

(24) $I_{D_{20}} = SR(C_1 + C_L) = 2\ (1 + \frac{C_L}{C_1}) \times I_{D_{16,17}}$

Using:

(25) $g_m = 2\sqrt{K_{n,p}(\frac{W}{L})I_D}$

And,

(26) $K_{n,p} = \frac{\mu_{n,p} C_{ox}}{2}$

The aspect ratio of the M_{16} and M_{17} transistors therefore can be calculated by

(27) $\left(\frac{W}{L}\right)_{16,17} = \frac{{g_{m_{16,17}}}^2}{4K_N\, I_{D_{16,172}}}$

The amplifier has a single second pole at the frequency determined by

(28) $f_{SP} = \frac{{g_{m_{19}}}^2}{4K_p\, I_{D_{20}}}$

Which leads to phase margin:

(29) $M_\Phi = 90° - arctan\,(\frac{f_{GBW}}{f_{SP}})$

A separation factor, K can be defined as tangent of the phase margin.

From the formulas above the transconductance gain of M_{19} can be calculated as

(30) $g_{m_{19}} = 2\pi f_{GBW} C_L tan(M_\Phi)$

And since the drain currents of M_{19} and M_{20} are identical, the aspect ratio of M_{19} is calculated as:

(31) $\left(\frac{W}{L}\right)_{19} = \frac{{g_{m_{19}}}^2}{4K_p I_{D_{20}}}$

To calculate the aspect ratio of transistors M_{12} and M_{11}, since they have the same V_{DS} it is observed that

(32) $V_{GS_{12}} = V_{DS_{11}} = V_{GS_{19}}$

(33) $\left(\frac{W}{L}\right)_{12,11} = \frac{I_{D_{11,12}}}{I_{D_{19}}}\left(\frac{W}{L}\right)_{19}$

To compensate for the right half-plane zero caused by the forward path to the output the resistance R1 and capacitance C1 are measured by:

(34) $R_1 = \frac{1}{g_{m_{19}}}$

(35) $$C_1 = K\frac{g_{m_{16,17}}}{g_{m_{19}}}C_L$$

Based on the mentioned calculations, the values and dimensions of the design components of the op-amp are shown in figure 32.

Low Pass Filter

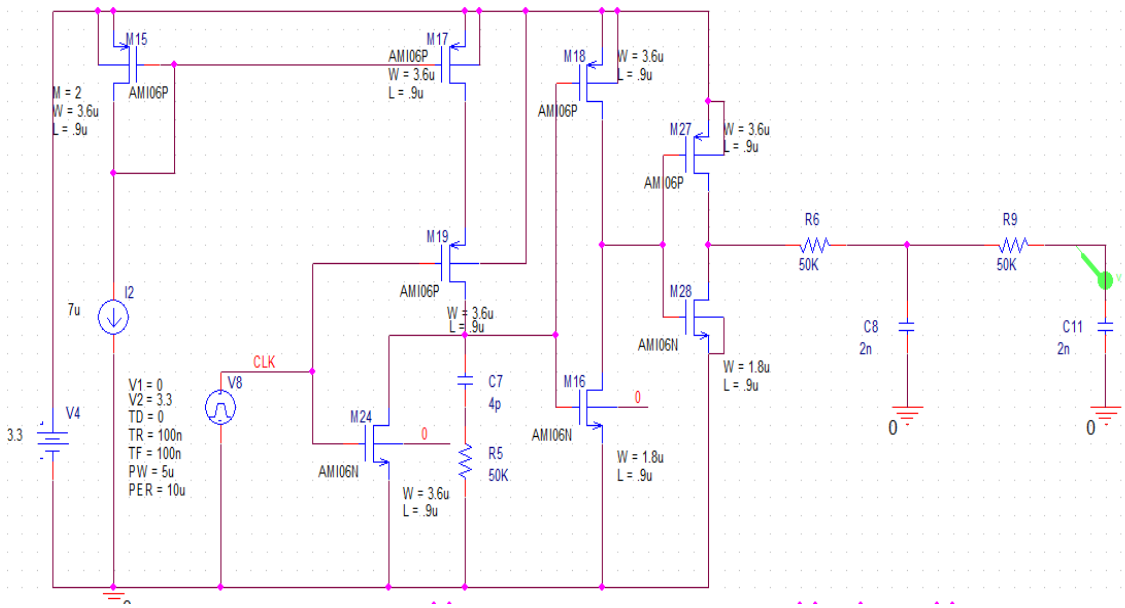

Figure 33: Low pass filter

The low-pass filter is a device that allows passing the dc component and low frequency contents of the input signal and attenuates the high frequency contents. Thus, the output of the filter circuit will be a steady dc voltage.

Figure 33 depicts the two passive RC, low pass filters used to filter the outcoming signal from the detection circuit. The filters are used to extract the DC content of the detection signals. In figure 32, $R_5 = 50k\Omega$ which means there are no bacteria present. A same circuit was simulated with $R_5 = 400k\Omega$ to demonstrate the detection of bacteria. In figure 34, the upper red trace shows the DC content of "detected bacteria" signal by 1.6v and the 1.1v shows the absence of bacteria.

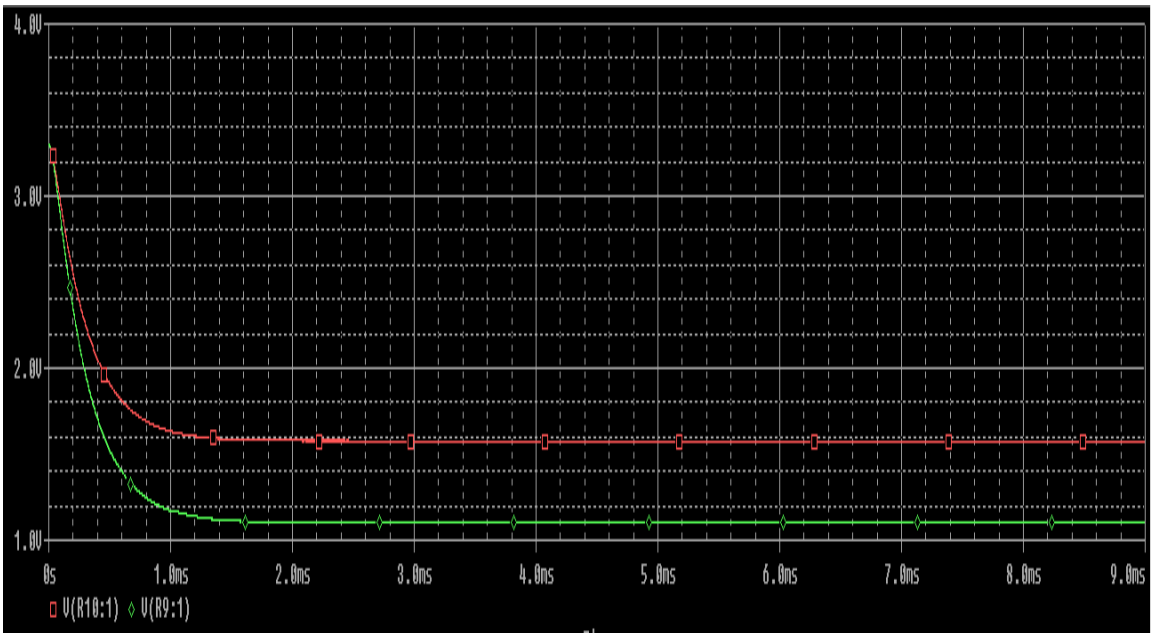

Figure 34: DC content of the detection signals

The Bode plots of the filter are shown in figure 35.

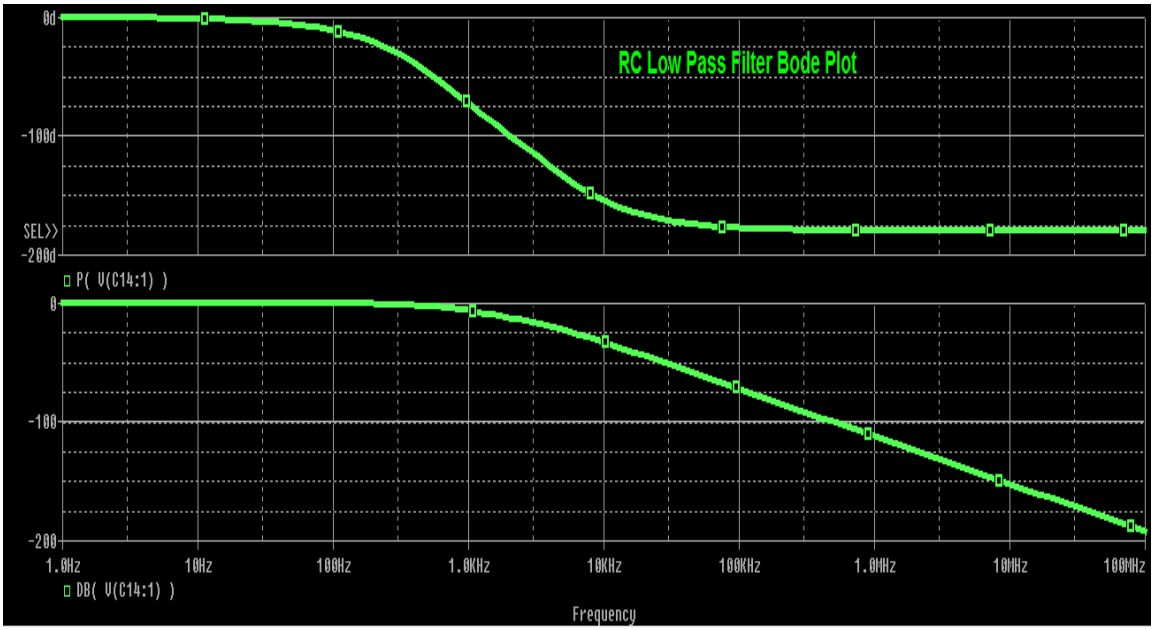

Figure 35:RC low pass filter Bode plots

Decision Circuit

The Schematics for the decision circuit is shown in figure 36. The core of the decision circuit is bistable element, created using cross-coupled PMOS pair (XCP) in a differential buffer. When the output of the low pass filter from the previous stage is higher than the 1.45v reference voltage created by the bandgap voltage reference, the output of the latch is pulled down. On the other hand, if the input is less than 1.45v the output is pulled high. The resulting signal is now a digital signal that is routed through inverters to LED driver circuits. LED driver circuits include a common drain transistor and a current limiting resistor. In the case shown in figure 36, the LED is depicted with a diode connected BJT.

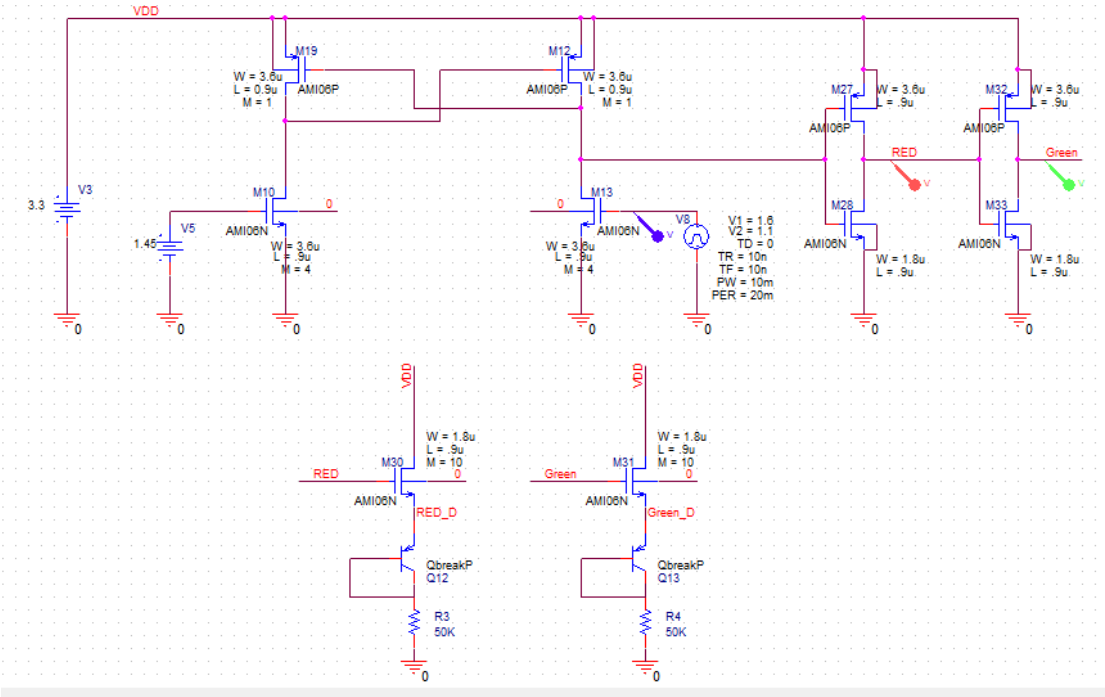

Figure 36: The comparator schematic

The output of the decision circuit is depicted in figure 37. The blue trace is signal detected from the passive low pass filter, where the wider the pulse width, the more impedance hence bacteria was detected. Both green and red traces swing between 3.3v

and 0v. If the green trace is high, bacteria has not been detected and as shown in the decision circuit schematic in figure 36, a green LED will be on. The same is true for red, which represents the presence of bacteria in the solution.

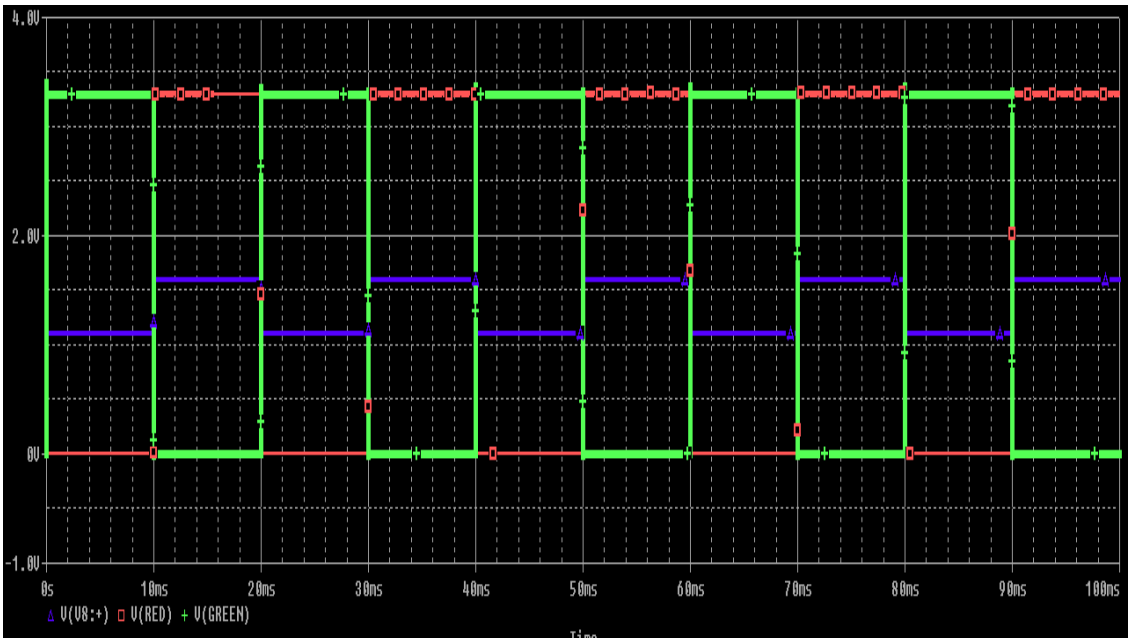

Figure 37: Decision circuit's output

CONCLUSION

The Vibrio Cholerae bacteria is the bacteria that causes the deadly Cholera disease. The bacteria cause an infection in small intestine which, if not detected early leads to severe dehydration, shock and death. Vibrio Cholera bacterium's cell has magnetosome. the magnetosome gives the bacteria cell an electrical property. This thesis extended a novel approach to detect bacteria using a lab on chip design that senses the change in impedance of sample solution as the result of bacteria's presence. The design included a temperature independent current reference, bandgap voltage and a main detection and decision circuits using On-Semi 500n process. An accurate, portable, low cost, low power and highly miniaturized lab system-on-a chip with an easy to manipulate output was designed, moving this platform closer to practical third world use.

REFERENCES

1. "Cholera - Vibrio cholerae infection." *Centers for Disease Control and Prevention*, Centers for Disease Control and Prevention, 9 Nov. 2016, www.cdc.gov/cholera/general/index.html.

2. "Cholera." *UNICEF*, 8 July 2016, www.unicef.org/cholera/index_81574.html.

3. *WHO | Global Health Observatory | Map Gallery*, World Health Organization, 2016, gamapserver.who.int/mapLibrary/app/searchResults.aspx.

4. Schauer, S., Sommer, R., Farnleitner, A. and Kirschner, A. (2017). *Rapid and Sensitive Quantification of Vibrio cholerae and Vibrio mimicus Cells in Water Samples by Use of Catalyzed Reporter Deposition Fluorescence In Situ Hybridization Combined with Solid-Phase Cytometry.* American Society of Microbiology. Available at: http://aem.asm.org/content/78/20/7369.full.

5. Mayoclinic.org. (2017). *Cholera - Diagnosis and treatment - Mayo Clinic*. Available at: http://www.mayoclinic.org/diseases-conditions/cholera/diagnosis-treatment/treatment/txc-20311193.

6. Huq, Anwar et al. "Detection, Isolation, and Identification of *Vibrio Cholerae* from the Environment." *Current protocols in microbiology* CHAPTER (2012): Unit6A.5. *PMC*. Web. 15 May 2017.

7. Dr Ananya Mandal, M. (2017). *Cholera Diagnosis*. [online] News-Medical.net. Available at: https://www.news-medical.net/health/Cholera-Diagnosis.aspx

8. Bacteriainphotos.com. (2017). *Vibrio cholerae colony morphology on TCBS*. Available at: http://www.bacteriainphotos.com/vibrio_cholerae_colony_morphology.html.

9. Aryal, S. (2017). *Thiosulfate-Citrate-Bile Salts-Sucrose (TCBS) Agar-Composition, Principle, Uses, Preparation and Colony Morphology - Online Microbiology Notes*. [online] Online Microbiology Notes. Available at: https://microbiologyinfo.com/thiosulfate-citrate-bile-salts-sucrose-tcbs-agar-composition-principle-uses-preparation-and-colony-morphology/.

10. Ley B, Khatib AM, Thriemer K, von Seidlein L, Deen J, Mukhopadyay A, et al. (2012) Evaluation of a Rapid Dipstick (Crystal VC) for the Diagnosis of Cholera in Zanzibar and a Comparison with Previous Studies. PLoS ONE 7(5): e36930. https://doi.org/10.1371/journal.pone.0036930

11. Schauer, S., Sommer, R., Farnleitner, A. and Kirschner, A. (2017). *Rapid and Sensitive Quantification of Vibrio cholerae and Vibrio mimicus Cells in Water Samples by Use of Catalyzed Reporter Deposition Fluorescence In Situ Hybridization Combined with Solid-Phase Cytometry*. [online] American Society of Microbiology. Available at: http://aem.asm.org/content/78/20/7369.full.

12. Lefèvre, Christopher T., and Dennis A. Bazylinski. “Ecology, Diversity, and Evolution of Magnetotactic Bacteria.” *Microbiology and Molecular Biology Reviews : MMBR* 77.3 (2013): 497–526. *PMC*. Web. 20 May 2017

13. De Angelis, K. (2017). *Microbiology 480-Spring 2017*. [online] Slideshare.net. Available at: https://www.slideshare.net/KristenDeAngelis/lecture-17-3-312016-slides

14. J. El Fouladi, Z. Lu, Y. Savaria and S. Martel, "An Integrated Biosensor for the Detection of Bio-entities Using Magnetotactic Bacteria and CMOS Technology," *2007 29th Annual International Conference of the IEEE Engineering in Medicine and Biology Society*, Lyon, 2007, pp. 119-122.doi: 10.1109/IEMBS.2007.4352237

15. Zhao Lu, J. El-Fouladi, S. Martel and Y. Savaria, "A hybrid bacteria and microparticle detection platform on a CMOS chip: Design, simulation and testing considerations," *2008 IEEE 14th International Mixed-Signals, Sensors, and Systems Test Workshop*, Vancouver, BC, 2008, pp. 1-7.doi: 10.1109/IMS3TW.2008.4581598

16. Meera Senthilingam and Puja Bhattacharjee, C. (2017). *Cholera cases in Yemen could reach 1 million this year*. [online] CNN. Available at: http://www.cnn.com/2017/09/29/health/cholera-outbreak-unrest-yemen-congo-bangladesh/index.html.

17. Gray, P., Hurst, P., Lewis, S. and Meyer, R. (2011). *Analysis and design of analog integrated circuits*. 5th ed. New York: Wiley, Chapter 4.

18. Day, M. (2017). *Understanding Low Drop Out (LDO) Regulators*. [online] Ti.com. Available at: http://www.ti.com/download/trng/docs/seminar/Topic%209%20-%20Understanding%20LDO%20dropout.pdf.